

INTERNATIONAL CENTRE FOR MECHANICAL SCIENCES

COURSES AND LECTURES - No. 373



DISCRETE STRUCTURAL OPTIMIZATION

EDITED BY

W. GUTKOWSKI
POLISH ACADEMY OF SCIENCES



SpringerWienNewYork

Le spese di stampa di questo volume sono in parte coperte da
contributi del Consiglio Nazionale delle Ricerche.

This volume contains 91 illustrations

This work is subject to copyright.

All rights are reserved,
whether the whole or part of the material is concerned
specifically those of translation, reprinting, re-use of illustrations,
broadcasting, reproduction by photocopying machine
or similar means, and storage in data banks.

© 1997 by CISM, Udine

Printed in Italy

In order to make this volume available as economically and as
rapidly as possible the authors' typescripts have been
reproduced in their original forms. This method unfortunately
has its typographical limitations but it is hoped that they in no
way distract the reader.

ISBN 3-211-82901-6 Springer-Verlag Wien New York

Chapter 4

BACKTRACK METHOD WITH APPLICATIONS TO DSO

J. Farkas and K. Jármai

University of Miskolc, Miskolc, Hungary

ABSTRACT

The backtrack discrete mathematical programming method is described giving a detailed flow chart. If a continuous mathematical method is used and discrete series of values are given for variables, the discrete optima can be determined by a complementary discretization which is also explained. Optimum design problems of stiffened and cellular plates, tubular trusses, welded box beams and welded steel silos are treated. In these applications the discrete variables appear in various forms. In the cost function the material and fabrication (welding) costs are formulated. It is shown that the optimum number of ribs in stiffened or cellular plates depends on the fabrication cost factor. In the optimization of trusses it is verified that the use of the Euler buckling formula gives unsafe solutions and the optimum geometry depends on the profile shape of compression members. In the multiobjective optimization of welded box beams the deflection is formulated as the third objective function in addition to the cost and weight functions. The systematic incorporation of the cost analysis in the optimization procedure is shown in the case of a welded steel silo. The detailed strength and cost calculation is carried out for the main structural parts of a silo for several discrete values of the height/diameter ratio to find the optimum one.

4.1 INTRODUCTION

A structure should be safe and economic. These two, in most cases conflicting aspects can be systematically synthesized by optimum design. Economy is achieved by minimizing the cost function and safety is guaranteed by considering the design constraints. The optimum design procedure has three main phases as follows:

- (1) *preparation*: selection of materials, profiles, type of structure, joints, fabrication technology, erection method, definition of loads, design constraints and objective function(s), definition of the candidate structural versions;
- (2) *mathematical phase*: constrained function minimization by computerized mathematical programming methods;
- (3) *evaluation*: selection of the most suitable structural versions adding some heuristical aspects (aesthetics, transportation etc.), investigation of the most significant parameters, sensitivity, working out design rules and incorporation into expert system(s).

Optimum design is important tool for engineers, since it enables them to *achieve significant weight and cost savings* by using mathematical methods and by systematization of the design process selecting all the important aspects.

In order to make a survey of the most important design problems for welded metal structures we start from the fact that the best way to decrease the weight of a plated structure is *the decrease of plate thicknesses*. In design of thin-walled structures a lot of problems arise as follows:

- (1) *fabrication difficulties* caused by residual welding stresses and distortions;
- (2) *stability problems*: overall and local buckling phenomena and their interaction;
- (3) *high additional stresses due to warping torsion*: it is necessary to apply the strength theory of thin-walled structures;
- (4) *high stress concentrations in joints*: danger of *fatigue fracture* in the case of variable loads;
- (5) *vibrations* due to low eigenfrequencies of a thin-walled structure: it is necessary to study the *vibration damping methods*;
- (6) to avoid buckling and vibration, *stiffeners* should be used and *stiffened plates and shells* should be designed;
- (7) determination of the sufficient measure of the decrease of plate thicknesses by *optimum design*.

The above mentioned aspects emphasize the need to study the optimum design which is the main theme of this course.

The variables in the optimum design of welded metal structures are as follows: *in rod structures* the dimensions of profiles (widths and thicknesses of plate elements of welded I- and box-beams), *in trusses*: the coordinates of nodes, cross-sectional areas of members, number of members; *in stiffened plates and shells*: dimensions of plate or shell elements, number of stiffeners. These variables can be treated as continuous or discrete. The dimensions of plate elements or standard profiles can be given by a series of discrete values. In this case we can treat them as discrete variables or as continuous ones and, at the end of optimization we can discretize them by an additional procedure. Thus, methods of discrete

or continuous optimization can be used. The advantage of a method depends on the optimization problem as it will be shown by applications.

In the following we show a selection of applications.

In the case of *stiffened plates* the main variable is the number of stiffeners which depends on the fabrication cost factor. In the optimization of a cellular plate several mathematical methods have been compared regarding their efficiency.

In the optimization of a *tubular truss* the overall and local buckling constraints have been important and the optimum structural height (distance between parallel chords) is sought which minimizes the whole weight. The overall buckling constraints should be defined according to the Eurocode 3 which considers the effect of initial imperfections of rods, since the calculation with the Euler formula gives errors in the unsafe side.

In the optimization of a *roof truss* it was shown that, due to the differences between the radii of gyration of various profiles used in compression members, the optimum roof slope angle depends on the type of profile. The optima have been found by calculating the weights corresponding to the series of discrete slope angles.

In the *multiobjective optimization of a welded box beam* three objective functions have been defined and several mathematical methods have been used.

The study of a *welded steel silo* illustrates how to synthesize the strength calculations with the fabrication cost analysis to find the optimum height/diameter ratio. The main structural parts of the silo are designed and the material and fabrication costs are calculated for discrete series of height/diameter-ratio.

4.2 THE BACKTRACK METHOD

The backtrack method is a combinatorial programming technique, solves nonlinear constrained function minimization problems by a systematic search procedure. The advantage of the technique, that it uses only discrete variables, so the solution is usable. The general description of backtrack can be found in the works of Walker [4.1], Golomb & Baumert [4.2] and Bitner & Reingold [4.3]. This method was applied to welded girder design by Lewis [4.4] and Annamalai [4.5]. Farkas & Szabó [4.6] have used it for the minimum cost design of hybrid I-beams. An estimation procedure for efficiency of backtrack programming was proposed by Knuth [4.7]. In the book of Farkas [4.8] the following problems have been solved by backtrack method: welded I-beam subject to bending, compression struts of square hollow section, a tubular truss, hybrid I-beams with one welded splices on the flanges, welded box beams subject to bending and shear, a crane runway girder of asymmetrical I-section, closed press frames of welded box section.

The general formulation of a single-criterion nonlinear programming problem is the following:

$$\text{minimize} \quad f(x) \quad x_1, x_2, \dots, x_N \quad (4.2.1)$$

$$\text{subject to} \quad g_j(x) \leq 0, \quad j = 1, 2, \dots, P \quad (4.2.2)$$

$$h_i(x) = 0 \quad i = P+1, \dots, P+M \quad (4.2.3)$$

$f(x)$ is a multivariable nonlinear function, $g_j(x)$ and $h_i(x)$ are nonlinear inequality and equality constraints. The equality constraints should transfer to inequality ones to handle them by the program:

$$\begin{aligned} h_i(x) - \varepsilon &\leq 0 \quad i = P+1, \dots, P+M \\ h_i(x) - \varepsilon &\geq 0 \end{aligned} \quad (4.2.4)$$

ε is a given small number.

The algorithm is suitable to find optimum of those problems which are characterized by monotonically increasing or decreasing objective functions. Thus, the optimum solution can be found by increasing or decreasing the variables. Originally the procedure can find the minimum of the problem. If we are looking for maximum, we should introduce $-f(x)$. The time of search is long, because the procedure makes a detailed search.

To find the optimum for a single variable many single variable search techniques are available. An efficient and suitable search method is the interval halving procedure.

We assume that the objective function is monotonously decreasing, if the variables are decreasing. At the line search, when only one variable is changing, the aim is to find the minimum feasible value of the variable, starting from the maximum value.

The starting point, i.e. the maximum value, should satisfy the constraints. When the investigation shows, that the minimum value satisfies the constraints, then the solution is found. If not, the region is divided into two subregions with the middle value. If the constraints are satisfied with the middle value, then the upper region is feasible, all points there satisfy the constraints. In this case we should investigate the lower region, to find the border between the feasible and unfeasible regions.

Sign [means feasibility, sign { unfeasibility. The halving procedure works as follows:

Assume, that the variable is a thickness given by the following series of discrete values:

6 8 10 12 15 18 20 25 30 mm
 { }

Furthermore assume that the maximum value is feasible, the minimum is unfeasible. If the middle value is feasible, the region to be investigated is as follows:

6 8 10 12 15
 { }

At the upper part of the region one cannot find any solution, so it is possible only at the lower part. We can leave the upper region without any further calculations. Continuing with the middle point of the lower region, if it is unfeasible, then the remaining region is only one quarter of the original one, after two checks.

10 12 15
 { }

If the middle point is feasible, then it gives the solution.

12
]

The ratio of the number of total discrete points and checked discrete values is $9 / 4$. If we have 1025 discrete values, then this ratio is much better, at the first halving step we can leave 512 discrete numbers without further investigations. The halving procedure stops, if

the step length is less, that the distance between two discrete points. The step length should not be uniform between every discrete values, but for practical reasons we usually use a uniform value. The number of discrete values should be 2^k+1 , where k is an integer number. In the case of a completely general series the latter can be completed with the maximum values as follows:

Basic:	1	2	3	4	5	6	7	8	9
Completed:	4	6	8	10	12	14	16	16	16

At the backtrack method the variables are in a vector form $x = \{x_j\}^T$ ($j = 1, \dots, n$) for which the objective function $f(x)$ will be a minimum and which will also satisfy the design constraints $g(x) \geq 0$ ($j = 1, \dots, P$). For the variables, series of discrete values are given in an increasing order. In special cases the series may be determined by $x_{k,\min}$, $x_{k,\max}$ and by the constant steps Δx_k between them. The flow chart for the backtrack method is given in Fig. 4.2.1.

First a partial search is carried out for each variable and if all variations have been investigated, a backtrack is made and a new partial search is performed on the previous variable. If this variable is the first one: no variations have to be investigated (a number of backtracks have been made), then the process stops. The main phases of the calculation are as follows.

1. With a set of constant values of $x_{i,l}$ ($i = 2, \dots, n$) the minimum $x_{i,m}$ value satisfying the design constraints is searched for. The interval halving method can be employed. This method can be employed if the constraints and the objective function are monotonous from the sense of variables.
2. As in the case of the first phase, the halving process is now used with constant values, and the minimum $x_{i,m}$ value, satisfying the design constraints is then determined.
3. The least value $x_{n,m}$ is calculated from the equation relating to the objective function $f(x)$

$$f(x_{1,m}, \dots, x_{n,m}) = f_o$$

where f is the value of the cost function calculated by inserting the maximum x -values. Regarding the $x_{n,m}$ value, three cases may occur as follows.

(3a) If we decrease x_{n-1} step-by step till it satisfies the constraints or till $x_{n,\min}$, the minimal values are reached. If all variations of the x_n value have been investigated, then the program jumps to the x_{n-1} and decreases it step-by step till x satisfies the constraints or till $x_{n-1,\min}$ are reached.

(3b) If $x_{n,m} \leq x_{n-1}$, we backtrack to x_{n-1} .

(3c) If $x_{n,m}$ does not satisfy the constraints, we backtrack to $x_{n-1,m}$. If the constraints are satisfied, we continue the calculation according to 3a.

The number of all possible variations is $\prod_{i=1}^n t_i$ where t_i is the number of discrete sizes for one variable. However, the method investigates only a relatively small number of these. Since the efficiency of the method depends on many factors (number of unknowns, series of

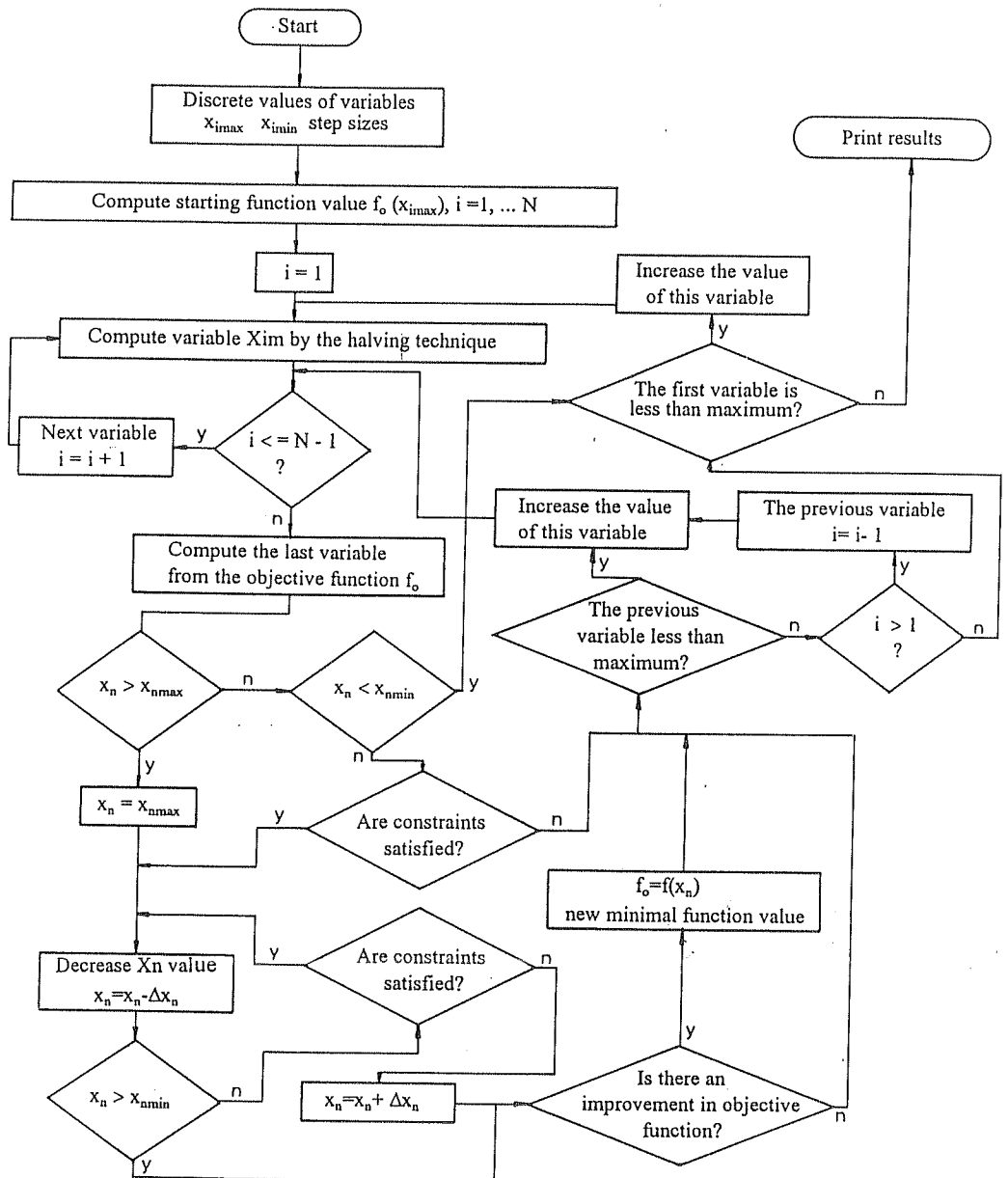


Fig.4.2.1. Flow chart of the backtrack method

discrete values, position of the optimum values in the series, complexity of the cost function and/or that of the design constraints), it is difficult to predict the run time. The main disadvantage of the method is, that the runtime increases exponentially, if we increase the number of unknowns.

We've made the program in C language modifying the procedure in the sense, that originally the program depended on the number of variables. All variables were computed by the halving procedure except the last one, which was computed from the objective function. The modified version is independent from the number of variables. Advantage of the method is, that it gives discrete values, usually finds global minimum. The disadvantage of the method that it is useful only for few variables because of the long computation time.

4.2.1. AN EXAMPLE OF USING BACKTRACK FOR SOLVING A COMBINATORIAL PROBLEM

A simple example to show the procedure in details is to place four queens on a four by four chess table not to beat each other.

The objective of the problem is to maximize the number of queens. The constraints are that the queens beat each other if they are at the same row, or column, or every row means one variable, one queen, because it is not possible to place two queens in the same row.

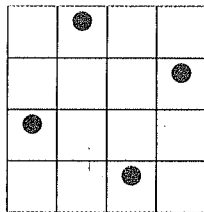
We can place the first queen, can find the place of the second queen, but no place for the third queen.

●			
		●	
X	X	X	X

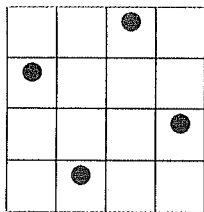
If there is no place for the third variable, we jump back to the second one and look for another place for it. Finding the next place, we can place the third variable too. Unfortunately there is no place for the fourth queen.

●			
			●
	●		
X	X	X	X

We have investigated all variations at the third variable, so we should jump back to the second variable, but there are no new possibilities, so should backtrack to the first variable and replace it. This case we can get a solution, which means, that we could place the maximum queens on the chess table, it is four and they don't beat each other, so satisfy the constraints.



There are more solutions like the following.



The discrete value of the method is that to place the queens on the chess table is possible only in the squares, it means that for a technical variable also a limited number of discrete values are given.

4.2.2. AN EXAMPLE OF USING BACKTRACK FOR OPTIMUM DESIGN OF A WELDED I-BEAM

The problem is finding the minimum mass solution of a welded I-beam, which is simply supported, subject to bending moment and shear force.

The unknowns are the height of web plate $h = x_1$, the thickness of web $t_w = x_2$, the area of the flange $A_f = x_3$.

The objective function is the mass of the structure. The span length is given, the material is also known (normal steel), so the minimum mass is equal to the minimum area of cross-section.

$$f(x) = x_1 x_2 + 2x_3$$

The design constraints are as follows:

$$g_1(x) \text{ is the normal stress constraint } \sigma_b + \sigma_c = \frac{M_b}{W_x} + \frac{N}{A} \leq R_u$$

where M_b is the bending moment,

N is the compression force,
 W_x is the section modulus,
 A is the cross-section area,
 R_u is the ultimate limit stress.

$$g_2(x) \text{ is the buckling constraint } \frac{h}{t_w} = 145_4 \sqrt{\frac{(1 + \frac{\sigma_c}{\sigma_b})^2}{1 + 173(\frac{\sigma_c}{\sigma_b})^2}}$$

Data are as follows:

$$M_b = 320 \text{ kNm}; \quad N = 128 \text{ kN}; \quad R_u = 200 \text{ MPa}$$

The upper and lower limits and step length is shown in Table 4.2.1. The numerical calculation is given in Table 4.2.2.

Table 4.2.1. Upper and lower limits of the variables

	Upper	Lower	Step length
h	740	660	20
t_w	9	5	1
A_f	2200	1400	100

Results are $h = 700 \text{ mm}$; $t_w = 6 \text{ mm}$; $A_f = 1800 \text{ mm}^2$

During the procedure the minimum function value and its variable values are saved and at the end of the procedure the final results come from these saved values. The search is not a direct one. If the second values give the solution it will continue the search till there are no possibilities for backtracking, jumping back for the previous variable and try to reduce the objective function value.

4.3 DISCRETIZATION AFTER CONTINUOUS OPTIMIZATION

To make the search more practicable it is advisable to use discrete member sizes. The original program was extended with a secondary search to find discrete optimum sizes in such a way, that not only the explicit and implicit constraints satisfied are but the merit function takes its minimum as well. It is assumed that the optimum discrete sizes are near to the optimal continuous ones [4.9].

Starting from the optimum continuous values, the secondary search chooses the nearest discrete sizes for each continuous size from the series of discrete values. The number of chosen discrete sizes for one continuous size can be two, three or more. The possible variations can be obtained using binary, ternary or larger systems. In our numerical example we use the binary system, two discrete sizes, upper and lower, belonging to one continuous value. In a binary system number the figure zero means the upper discrete size, the figure

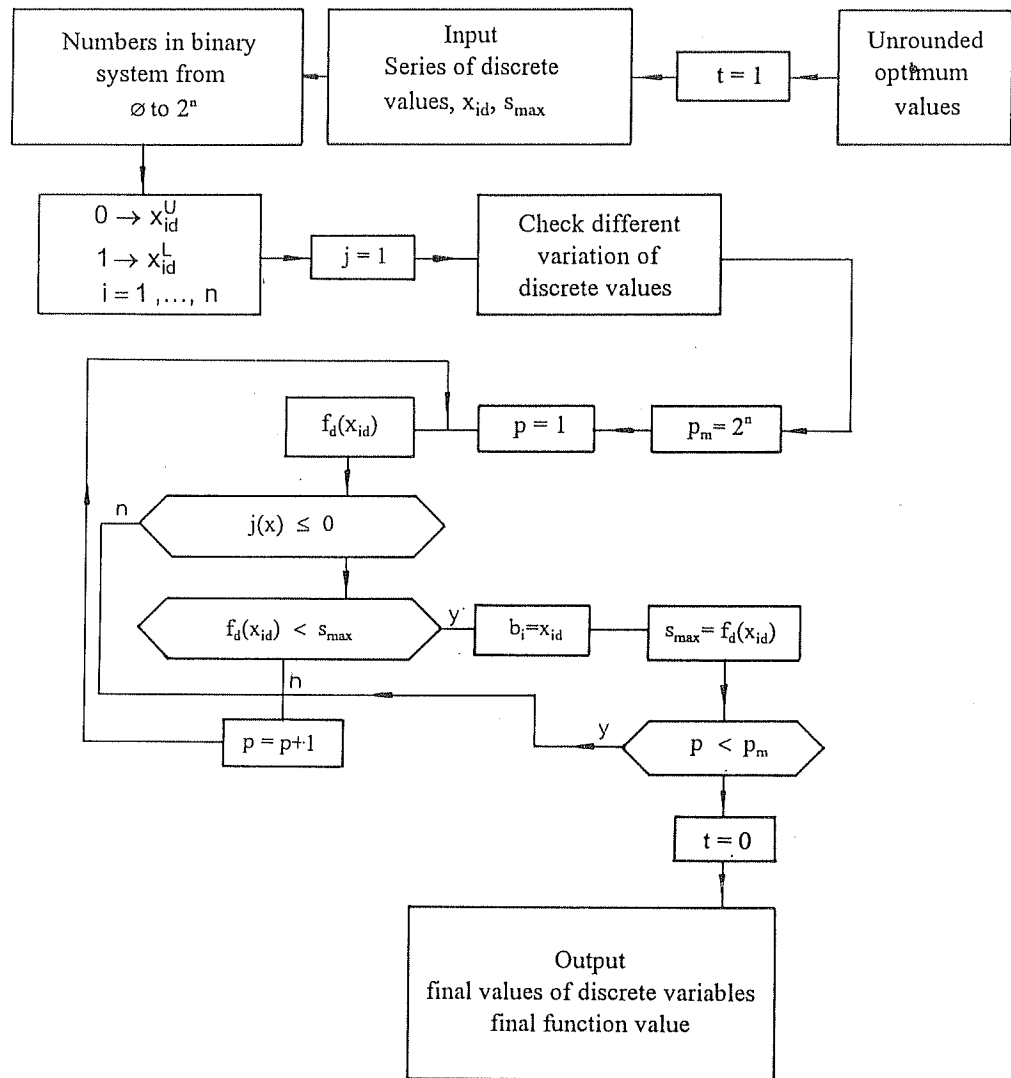


Fig.4.3.1. Discretization after continuous optimization

one means the lower one. The first $2n$ number in binary system gives the all possible variations. Each variation is tested, whether the explicit and implicit constraints are satisfied, and the optimal values minimizing the merit function are determined. (Fig. 4.3.1).

The unrounded optimum values of fourth variable are as follows: ♣ ♦ ♥ ♠

Lower	♣	Upper
Lower	♦	Upper
Lower	♥	Upper
Lower	♠	Upper

The number 0000 means the lower discrete values of all variables, the number 1111 means the upper discrete values of all variables. The other numbers in the binary system are the variants of the possible discrete solution. One of the tested variants is the solution, giving the minimum objective function value.

4.4 MINIMUM COST DESIGN OF LATERALLY LOADED WELDED RECTANGULAR CELLULAR PLATES

4.4.1 INTRODUCTION

A cellular plate consists of two parallel face sheets welded to an orthogonal grid of ribs sandwiched between them (Fig.4.4.1). This type of welded sandwich plates has the following advantages over plates stiffened on one side: *a./ the torsional stiffness is much larger, b./ the height of ribs can be much smaller, c./ fabrication imperfections due to the shrinkage of welds are much smaller because of the symmetry of the structure, d./ the planar surface can be more easily protected against corrosion.*

Cellular plates may be applied in ships, bridges, dock gates, light-weight roofs, elements of machine structures etc. Their disadvantage is that, if the rib height is smaller than approx. 800 mm, the face plates cannot be welded to ribs from inside. Then these connections can be realized from outside by arc-spot-welding, electron beam welding, slot or plug welds.

A brief survey of selected literature is given in [4.10]. The research has been carried out predominantly in the field of double bottoms of ships. The present paper is a generalization of the investigation of the minimum cost design of square cellular plates [4.10]. Our aim is to show how to optimize the plate dimensions, mainly the numbers of ribs. It will be shown by numerical examples the effect of fabrication costs and the yield stress of steel on the optimal number of ribs.

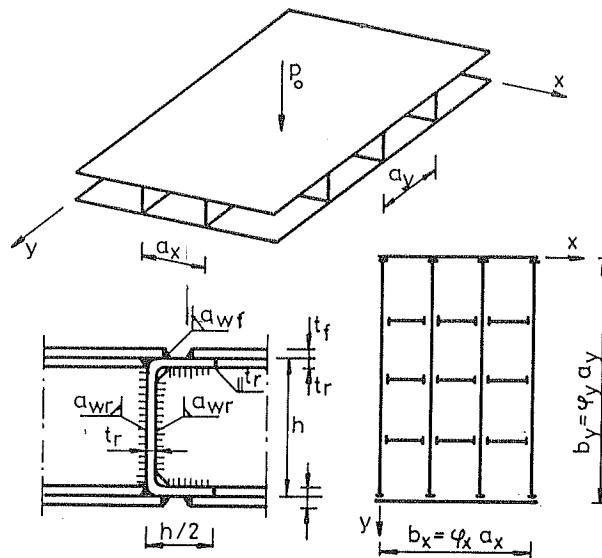


Fig.4.4.1. Details of a welded rectangular cellular plate

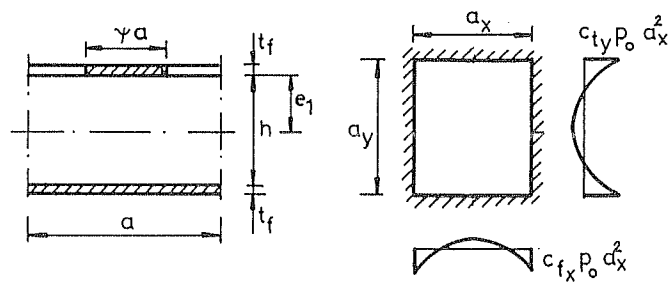


Fig.4.4.2.(a) Effective cross-section for calculation of the bending stiffness; (b) local bending of an upper plate element due to the uniformly distributed lateral load

4.4.2 THE COST FUNCTION

It is assumed that the fabrication has the following steps. First the grid of ribs is welded from cold-formed channels or from welded I-beams. The grid nodes should be completely welded to be able to carry bending moments and shear forces. Then the elements of the upper and lower cover plates are welded to the ribs from outside with fillet welds (Fig. 4.4.1). This method is selected since one cannot find cost data for other welding methods. The ribs are continuous in y direction and intermittent in x direction. The cross-sectional area of a rib is approx. $2ht_f$, where h is the height, t_f is the thickness. The integer numbers of rib distances are φ_x and φ_y , respectively (Fig. 4.4.1). The number of ribs in x - and y direction is $\varphi_x + 1$ and $\varphi_y + 1$, resp. Assuming that all ribs have the same cross-sectional area, the whole volume of the cellular plate is

$$V = 2b_x b_y t_f + 2b_x h t_{rx} (\varphi_y + 1) + 2b_y h t_{ry} (\varphi_x + 1) \quad (4.4.1)$$

where t_f is the thickness of face plates. The total cost consists of the material and fabrication costs

$$K = K_m + K_f = k_m \rho V + k_f \sum T_i \quad (4.4.2)$$

$$\text{or in other form } K / k_m = \rho V + k_f / k_m (T_1 + T_2 + T_3) \quad (4.4.3)$$

where k_m (\$/kg) and k_f (\$/min) are the material and fabrication cost factors, resp, ρ is the material density, T_i are the fabrication times in min.

In order to give internationally usable solutions, the following ranges of k_m and k_f may be considered. For steel Fe 360 $k_m = 0.5$ -1.2 \$/kg, for fabrication including overheads $k_f = 15$ -45 \$/manhour = 0.25-0.75 \$/min. Thus the ratio k_f/k_m may vary in the range 0-1.5 kg/min. The value $k_f/k_m = 0$ in (4.4.3) corresponds to the minimum volume design. For the calculation of times T_i we use the method proposed by Pahl and Beelich [4.11].

a./ Preparation, assembly and tacking

$$T_1 = C_1 \delta \sqrt{\rho V} \sqrt{\kappa}; \quad C_1 = 1.0 \text{ min/kg}^{0.5} \quad (4.4.4)$$

where Θ is a difficulty factor, κ is the number of structural elements to be assembled. Number of continuous ribs in y direction is $\varphi_y + 1$, number of rib elements in x direction (internal intermittent, peripheral continuous, Fig. 4.4.1) is $\varphi_x (\varphi_y - 1) + 2$, number of face plate elements is $2\varphi_x \varphi_y$. Thus the number of all structural elements is $\kappa = 3(\varphi_x \varphi_y + 1)$ and $T_1 = 3\sqrt{\rho V} \sqrt{3(\varphi_x \varphi_y + 1)}$

$$(4.4.5)$$

b./ Welding

$$T_2 = \sum C_{2i} a_{wi}^{1.5} L_{wi} \quad (4.4.6)$$

$C_2' = 0.8 \cdot 10^{-3} \text{ min/(mm}^{1.5}\text{mm)}$ for manual arc-welding $C_2'' = 0.5 \cdot 10^{-3} \text{ min/(mm}^{1.5}\text{mm)}$ for CO₂-welding a_{wi} and L_{wi} are the size and length of welds in mm, resp.

It is assumed that the grid nodes are joined by manual-arc-welding with fillet welds and the face plate elements are connected to the grid by CO₂-welded fillet welds.

c./ *Electrode changing, weld deslagging and chipping*

$$T_3 = \sum C_{3i} a_{wi}^{1.5} L_{wi}, \quad C_3' = C_2', \quad C_3'' = C_2'' \quad (4.4.7)$$

The number of perpendicular joints of ribs is

$$2(\varphi_x + 1) + 2 \varphi_x (\varphi_y - 1) = 2(\varphi_x \varphi_y + 1)$$

It is assumed that the webs of ribs are welded with fillet welds of size $a_w = 0.7 t_{ry}$ in the length of $2h$, and the flanges of ribs of length h are welded with welds of $a_w = t_{ry}$ (Fig.4.4.1). Thus the $T_2 + T_3$ times for manual-arc-welded nodes are (in min)

$$T_2' + T_3' = (1 + \sqrt{\Theta}) 0.8 \cdot 10^{-3} \cdot 2(\varphi_x \varphi_y + 1) [h t_{ry}^{1.5} + 2h (0.7 t_{ry})^{1.5}] \quad (4.4.8)$$

The total length of fillet welds for face plate elements is

$$2 \varphi_x \varphi_y (2a_x + 2a_y) = 4 \varphi_x \varphi_y (b_x / \varphi_x + b_y / \varphi_y)$$

and the fillet weld size is taken as $a_w f = 0.5 t_f$, thus

$$T_2' + T_3' = (1 + \sqrt{\Theta}) 0.5 \cdot 10^{-3} (0.5 t_f)^{1.5} 4 \varphi_x \varphi_y (b_x / \varphi_x + b_y / \varphi_y) \quad (4.4.9)$$

all sizes in mm.

4.4.3 THE DESIGN CONSTRAINTS

a./ *Constraints on compressive elastic stresses in the central upper face plate element are as follows*

$$\sigma_{x,max} + \sigma_{xf,max} \leq \sigma_{adm} \quad (4.4.10)$$

$$\sigma_{y,max} + \sigma_{yf,max} \leq \sigma_{adm} \quad (4.4.11)$$

where σ_{adm} is the admissible stress, $\sigma_{x,adm}$ and $\sigma_{y,adm}$ are caused by the bending of the whole plate, $\sigma_{xf,adm}$ and $\sigma_{yf,adm}$ are normal stresses due to the local bending of the face plate element.

It can be verified, similarly to the case of a square cellular plate [4.12] that, because of the large torsional stiffness of cells, the whole rectangular cellular plate can be calculated as an isotropic one.

$$\sigma_{x,adm} = M_{x,max} E_1 e_1 / B; \quad \sigma_{y,adm} = M_{y,max} E_1 e_1 / B \quad (4.4.12)$$

According to the isotropic plate theory [4.13]

$$M_{x,max} = c_{mx} p b_x^2 \text{ and } M_{y,max} = c_{my} p b_y^2$$

there $p = 1.1 p_0$, with the factor of 1.1 the self weight is considered, c_{mx} and c_{my} are given in [4.13] for simply supported edges. The bending stiffness B is calculated considering the effective width of the compressed face plate element (Fig.4.4.2.a)

$B = E_1 I / a = E_1 h^2 t_f \psi / (1 + \psi)$, $e_1 = h / (1 + \psi)$, $E_1 = E / (1 - \nu^2)$ (4.4.13) where E is the modulus of elasticity and ν is the Poisson's ratio.

We use here the effective width formula proposed by Usami and Fukumoto [4.14]

$$\psi = 0.75 / \lambda_p; \lambda_p = \frac{a}{t_f} \sqrt{\frac{12(1-\nu^2)\sigma_{\max}}{4\pi^2 E}} \quad \text{or} \quad \psi = 1.426 / \lambda_p; \lambda_p = \frac{a}{t_f} \sqrt{\frac{\sigma_{\max}}{E}} \quad (4.4.14)$$

Substitution of (4.4.13) into (4.4.12) yields

$$\sigma_{x,\max} = c_{mx} p b_x^2 / (t_f h \psi_y) \quad \text{and} \quad \sigma_{y,\max} = c_{my} p b_y^2 / (t_f h \psi_x) \quad (4.4.15)$$

Elimination of ψ from (4.4.15) is performed using (4.4.14) and (4.4.15) and yields

$$\begin{aligned} \sigma_{x,\max} &= c_{mx}^2 p^2 b_x^4 a_y^2 / (1.426^2 t_f^4 E h^2); \\ \sigma_{y,\max} &= c_{my}^2 p^2 b_y^4 a_x^2 / (1.426^2 t_f^4 E h^2) \end{aligned} \quad (4.4.16)$$

$$\text{Furthermore } \sigma_{xf,\max} = 6 c_{fx} p_0 a_x^2 / t_f^2, \quad \text{and} \quad \sigma_{yf,\max} = 6 c_{fy} p_0 a_y^2 / t_f^2 \quad (4.4.17)$$

where c_{fx} and c_{fy} are given in [4.13] for a uniformly loaded rectangular isotropic plate with clamped edges (Fig. 4.4.2.b). Since c_{fx} and c_{fy} vary during the optimization procedure these values are calculated with approximate analytical formulae in a polynomial form

$$c_{fx} = c_0 + c_1 a_y/a_x + c_2 (a_y/a_x)^2 + c_3 (a_y/a_x)^3$$

On the contrary, values of c_{mx} , c_{my} , c_{qx} and c_{qy} are constant during an optimization procedure, because b_y and b_x are given in a numerical example.

b./ Constraints on local buckling of rib webs due to bending

$$\sigma_{x,\max} \leq \frac{23.9\pi^2 E_1}{12\gamma_b} \left(\frac{t_{rx}}{h}\right)^2 \quad \text{and} \quad \sigma_{y,\max} \leq \frac{23.9\pi^2 E_1}{12\gamma_b} \left(\frac{t_{ry}}{h}\right)^2 \quad (4.4.18 \text{ a,b})$$

where γ_b is the safety factor for buckling.

c./ Constraints on local buckling of rib webs due to shear

$$\tau_x = \frac{Q_x a_y}{h t_{rx}} = \frac{c_{qx} p b_x a_y}{h t_{rx}} \leq \frac{5.34\pi^2 E_1}{12\gamma_b} \left(\frac{t_{rx}}{h}\right)^2; \quad \tau_x \leq \tau_{adm} \quad (4.4.19a)$$

$$\tau_y = \frac{Q_y a_x}{h t_{ry}} = \frac{c_{qy} p b_y a_x}{h t_{ry}} \leq \frac{5.34\pi^2 E_1}{12\gamma_b} \left(\frac{t_{ry}}{h}\right)^2; \quad \tau_y \leq \tau_{adm} \quad (4.4.19b)$$

where $\tau_{adm} = \sigma_{adm} \sqrt{3}$ is the admissible shear stress, c_{qx} and c_{qy} are given in [4.13].

d./ Size constraints are the thickness limitations

$$t_{rx} \geq t_0; \quad t_{ry} \geq t_0 \quad \text{and} \quad t_f \geq t_0 \quad (4.4.20)$$

where t_0 is the minimum thickness considering the welding technology. Note that the deflection constraint is not considered here because of the large stiffness of the whole cellular plate.

4.4.4 THE OPTIMIZATION PROCEDURE

In a numerical example the values of p_o , b_y , b_x , σ_{adm} , E , ν , c_{mx} , c_{my} , c_{qx} , c_{qy} , t_o are given, and the unknowns to be optimized for minimum cost K_{min} are as follows: φ_x , φ_y , h , t_f , t_{rx} and t_{ry} . In the cost function the k_f/k_m ratio is varied in the range of 0-1.5. For the purpose of comparison we have used here three mathematical programming methods.

a./ *The backtrack combinatorial method* is advantageous here, since the number of variables is only 6, φ_x and φ_y are integer numbers and the thicknesses should be commercially available, so the series of discrete values to be investigated can easily be defined. The starting point should be feasible.

b./ *The hillclimb method* is proposed by Rosenbrock. The method of rotating coordinates is a further development of the Hooke and Jeeves method. No derivatives are required. The starting point should be feasible. We have supplemented this method with a secondary search for finding discrete values after having continuous ones [4.9].

c./ *FSQP - feasible sequential quadratic programming - method*. CFSQP 1.0 is a set of C subroutines for the minimization of smooth objective functions subject to general smooth constraints [4.15]. If the initial guess provided by the user is unfeasible for some constraints, CFSQP first generates a feasible point. Nonlinear equality constraints are turned into inequality constraints. The user must provide subroutines that define the objective functions and constraint functions or require that CFSQP estimates them by forward finite differences. CFSQP solves a modified optimization problem with only linear constraints and nonlinear inequality constraints. An Armijo-type line search is used to generate an, initial feasible point when required. After obtaining feasibility, either an Armijo-type line search may be used or a nonmonotone line search is made and analysed. The C version is a quite new development and we have worked also with the beta version on PC.

All of the programs are written in C and run under Borland C++ on PC 486 type computer. These codes are quicker than the Fortran and Basic codes and are more transportable, we also could run them on workstation.

4.4.5 NUMERICAL EXAMPLES

Data: the intensity of the uniformly distributed normal load $p_o = 5 \cdot 10^{-3}$ N/mm², $p = 1.1 \cdot p_o = 5.5 \cdot 10^{-3}$ N/mm², $t_o = 2$ mm, $E = 2.1 \cdot 10^5$ MPa, $\nu = 0.3$, $\rho = 7850$ kg/m³, $\gamma_b = 2$, $\Theta = 3$, $b_x = 10$ m. To show the effect of yield stress of steel, calculations

are made for steel Fe 360 with $\sigma_{adm} = 120$ MPa, and for steel Fe 510 with $\sigma_{adm} = 120 \cdot 355 / 235 = 181$ MPa.

To show the effect of fabrication costs calculations are made for $k_f/k_m = 0; 0.5; 1.0$ and 1.5 . The results are shown in Figs 4.4.2-3 and Table 4.4.1. Fig. 4.4.2 shows the curves of the objective function as a function of x in the vicinity of the optimum value. It can be seen that for larger k_f/k_m values - larger fabrication costs $\varphi_{x,opt.}$ is smaller. With the use of higher-strength steel Fe 510 4-12 % cost savings can be achieved. The sensitivity of the objective function is small.

In Fig. 4.4.3 the minimum K/k_m cost values are plotted in function of b_y/b_x for steels Fe 360 and Fe 510. It can be seen that the K/k_m values vary with b_y/b_x approximately linearly.

These results are obtained by backtrack programming method.

In Table 4.4.1. the optimal dimensions obtained by three methods are given for a numerical example. It can be seen that the hillclimb and CFSQP methods resulted in very similar undiscretized optimal values. The results obtained by Hillclimb with discretization and by the discrete backtrack are also very similar.

Table 4.4.1. Results of a numerical example with $b_x = 10$ m, $b_y = 14$ m, steel Fe 360 obtained by three mathematical programming methods, dimensions in mm

Method	k_f/k_m	φ_x	φ_y	t_f	t_{rx}	t_{ry}	h	K/k_m (kg)
CFSQP	0	13.0	16.0	5.1	2.2	2.0	278	14548
without	0.5	12.8	16.0	5.1	2.2	2.0	285	23627
discre-	1.0	10.2	8.8	6.1	3.0	2.4	383	31743
tization	1.5	9.4	8.0	6.0	3.1	2.5	406	38705
hillclimb	0	13.1	15.7	5.0	2.3	2.0	299	14624
without	0.5	10.0	9.0	6.0	3.0	2.4	400	24609
discre-	1.0	10.0	8.0	6.0	3.2	2.5	499	31888
tization	1.5	8.0	7.9	7.0	3.1	2.6	374	39094
hillclimb	0	14.	15.	5.	3.	2.	300	15229
with	0.5	10.	9.	6.	3.	3.	400	25459
discre-	1.0	10.	8.	6.	4.	3.	450	33485
tization	1.5	8.	8.	7.	4.	3.	375	40665
backtrack	0	13.	16.	5.	3.	3.	300	16162
	0.5	10.	9.	6.	4.	3.	400	26149
	1.0	10.	8.	6.	4.	3.	450	33485
	1.5	8.	8.	7.	4.	3.	375	40665

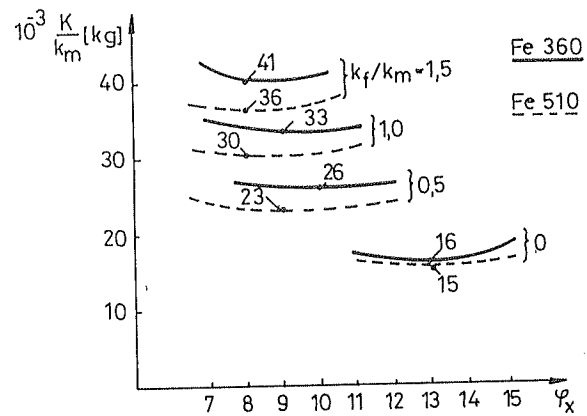


Fig.4.4.3. Results of a numerical example: minimum costs for various k_f/k_m ratios and the φ_{xopt} values

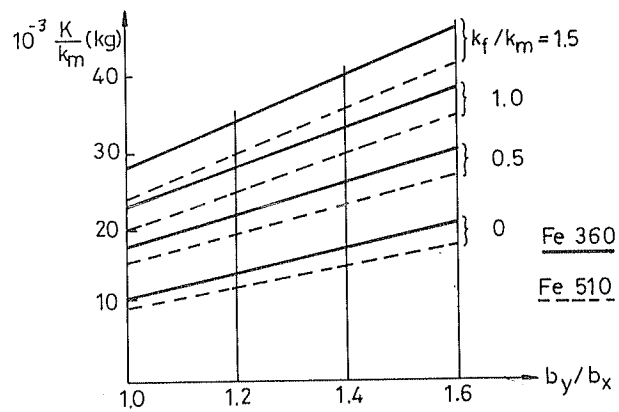


Fig.4.4.4. Result of a numerical example: : minimum costs for various k_f/k_m ratios in function of b_y/b_x

4.4.6 CONCLUSIONS

Illustrative numerical examples show that, because of the large torsional stiffness of cellular plates, relatively large structures can be realized using thin plates. The optimal number of ribs decreases when the fabrication cost k_f/k_m increases. The sensitivity of the objective function is small. The use of Fe 510 instead of Fe 360 results in 4-12 % cost savings. Active constraints are the normal stress limitation (4.4.10) and the constraints on local shear buckling of rib webs (4.4.19).

The comparison of the three mathematical programming methods shows that the hillclimb technique is quick but can result in local minima, the Backtrack is suitable for few variables defined by series of discrete values, the CFSQP method is very robust and the starting point can be unfeasible.

4.5 THE EFFECT OF WELDING TECHNOLOGIES IN THE DESIGN OF STIFFENED PLATES

4.5.1 INTRODUCTION

The economy of welded structures plays an important role in the research and production, therefore it is included in the work of IIW (International Institute of Welding) Commission XV. It needs a cooperation of designers and manufacturers, so it is a main task for the new Subcommittee XV-F "Interaction of design and fabrication".

In the recent publications [4.16, 4.17, 4.11] the first author has used a relatively simple cost function proposed by Pahl and Beelich [4.12]. These authors have given the production times only for SMAW (shielded metal arc welding) and GMAW-C (gas metal arc welding with CO₂). Their values have been modified [4.18] using some other publications [4.19].

To apply these cost calculations for another welding technologies, mainly for SAW (submerged arc welding), the COSTCOMP [4.20] software has been used [4.21]. The values of COSTCOMP enable us to define cost functions for different welding technologies. The aim of the present study is to apply the minimum cost design procedure for simple welded structures to show the advantage of automatic welding technology by cost comparisons.

4.5.2 THE COST FUNCTION

The cost calculation method described in Section 4.4.2 is modified according to Costcomp as follows:

$$T_2 = \sum_i C_{2i} \alpha_{wi}^n L_{wi} \quad (4.5.1)$$

is the time of welding, α_{wi} is the weld size, L_{wi} is the weld length, C_{2i} and n are constants given for different welding technologies.

$$T_3 = \sum_i C_{3i} \alpha_{wi}^n L_{wi} \quad (4.5.2)$$

is the time of additional fabrication actions such as changing the electrode, deslagging and chipping.

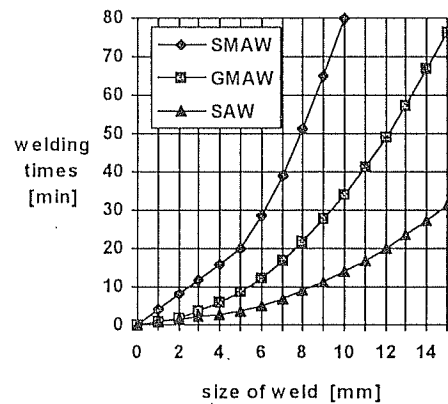


Fig. 4.5.1. Welding times for fillet welds of size α_w

Table 4.5.1. Welding times T_2 (min) in function of weld size α_w (mm) for longitudinal fillet welds downhand position (see also Fig. 4.5.1.)

Welding method	α_w (mm)	$10^3 T_2 = 10^3 C_2 \alpha_w^n$
SMAW	2 - 5	$4.0 \alpha_w$
	5 - 15	$0.8 \alpha_w^2$
GMAW-C	2 - 5	$1.70 \alpha_w$
	5 - 15	$0.34 \alpha_w^2$
SAW	2 - 5	$1.190 \alpha_w$
	5 - 15	$0.238 \alpha_w^2$

Ott and Hubka [4.19] proposed that $C_{3i} = 0.3 C_{2i}$, so

$$T_2 + T_3 = 1.3 \sum_i C_{2i} \alpha_{wi}^n L_{wi} \quad (4.5.3)$$

Values of C_{2i} and n may be given according to COSTCOMP [4.20] as follows. The COSTCOMP software gives welding times and costs for different technologies. To compare the costs of different welding methods and to show the advantages of automation, the manual SMAW, semi-automatic GMAW-C and automatic SAW methods are selected for fillet welds. The analysis of COSTCOMP data resulted in constants given in Fig. 4.5.1 and Table 4.5.1.

It should be noted that in values for SAW a multiplying factor of 1.7 is considered since in COSTCOMP different cost factors are given for various welding methods.

4.5.3 NUMERICAL EXAMPLE OF A STIFFENED PLATE

In order to show the effect of various welding methods on the optimal dimensions, weight and cost of a welded structure, an illustrative numerical example is chosen and the structural versions optimized for different welding methods are compared to each other.

Stiffened panels are widely used in bridge and ship structures, so it is of interest to study the minimum cost design of such structural elements. On the other hand, it has been shown [4.18] that the fabrication cost of a welded stiffened plate represents a significant part of the total cost.

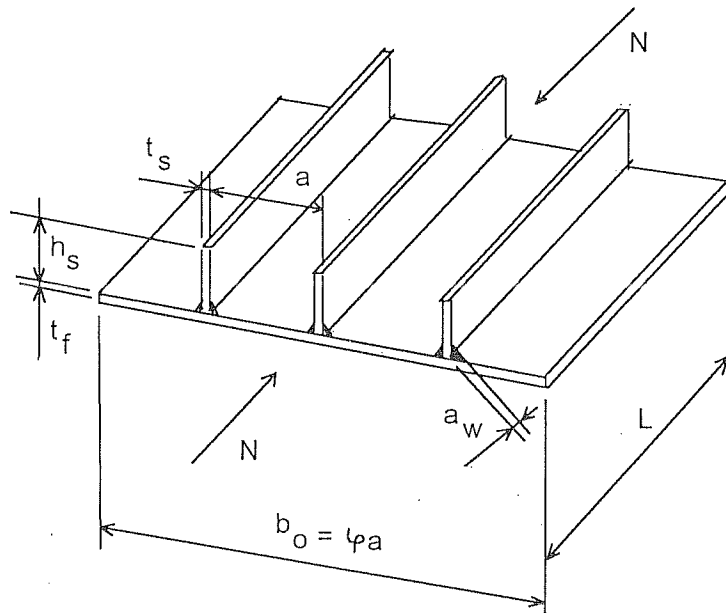


Fig. 4.5.2. Uniaxially compressed longitudinally stiffened plate

The design rules of *API* [4.22] are used here for the formulation of the global buckling constraint for uniaxially compressed plate longitudinally stiffened by equally spaced uniform flat stiffeners of equal cross sections (Fig. 4.5.2). The cost function is defined according to Section 4.5.2)

$$\frac{K}{k_m} = \rho LA + \frac{k_f}{k_m} (\Theta \sqrt{\kappa \rho LA} + 1.3 C_2 a_w'' L_w) \quad (4.5.4)$$

where $A = b_o t_f + \varphi h_s t_s$; $\Theta = 3$; $\kappa = \varphi + 1$; $L_w = 2L\varphi$; φ is the number of stiffeners.

The following ranges of k_m and k_f are considered. For steel Fe 360 $k_m = 0.5 - 1.2$ \$/kg, for fabrication including overheads $k_f = 15 - 45$ \$/manhour = 0.25 - 0.75 \$/min. Thus the ratio k_f/k_m may vary in the range 0 - 1.5 kg/min. The value $k_f/k_m = 0$ corresponds to the minimum weight design.

The flat stiffeners are welded by double fillet welds, the size of welds is taken as $a_w = 0.5 t_s$. The welding costs are calculated for SMAW, GMAW-C and SAW according to Table 4.5.1.

In the optimization procedure the given data are as follows. The modulus of elasticity for steel is $E = 2.1 \cdot 10^5$ MPa, the material density is $\rho = 7.85 \cdot 10^{-6}$ kg/mm³, the Poisson's ratio is $\nu = 0.3$, the yield stress is $f_y = 235$ MPa, the plate width is $b_o = 4200$ mm, the length is $L = 4000$ mm. The axial compressive force is

$$N = f_y b_o t_{fmax} = 235 \cdot 4200 \cdot 20 = 1.974 \cdot 10^7 \text{ [N]}$$

The variables to be optimized are as follows (Fig. 4.5.2): the thickness of the base plate t_f , the sizes of stiffeners h_s and t_s and the number of stiffeners $\varphi = b_o/a$.

The overall buckling constraint is given by

$$N \leq \chi f_y A \quad (4.5.5)$$

where the buckling factor χ is given in function of the reduced slenderness $\bar{\lambda}$

$$\chi = 1 \quad \text{for} \quad \bar{\lambda} \leq 0.5 \quad (4.5.6a)$$

$$\chi = 1.5 - \bar{\lambda} \quad \text{for} \quad 0.5 \leq \bar{\lambda} \leq 1 \quad (4.5.6b)$$

$$\chi = 0.5/\bar{\lambda} \quad \text{for} \quad \bar{\lambda} \geq 1 \quad (4.5.6c)$$

where

$$\bar{\lambda} = \frac{b_o}{t_f} \sqrt{\frac{12(1-\nu^2)f_y}{E\pi^2 k}} \quad (4.5.7)$$

$$k = \min(k_R, k_F); \quad k_R = 4\varphi^2 \quad (4.5.8a,b)$$

$$k_F = \frac{(1+\alpha^2)^2 + \varphi\gamma}{\alpha^2(1+\varphi\delta_p)} \quad \text{when} \quad \alpha = \frac{L}{b_o} \leq \sqrt{1+\varphi\gamma} \quad (4.5.8c)$$

$$k_F = \frac{2(1 + \sqrt{1 + \varphi\gamma})}{1 + \varphi\gamma} \quad \text{when} \quad \alpha \geq \sqrt{1 + \varphi\gamma} \quad (4.5.8d)$$

$$\delta_P = \frac{h_s t_s}{b_0 t_f}; \quad \gamma = \frac{EI_s}{b_0 D}; \quad I_s = \frac{h_s^3 t_s}{3}; \quad D = \frac{Et_f^3}{12(1 - \nu^2)} \quad (4.5.8e)$$

$$\text{so} \quad \gamma = 4(1 - \nu^2) \frac{h_s^3 t_s}{b_0 t_f^3} = 3.64 \frac{h_s^3 t_s}{b_0 t_f^3} \quad (4.5.8f)$$

I_s is the moment of inertia of one stiffener about an axis parallel to the plate surface at the base of the stiffener, D is the flexural stiffness of the base plate.

The constraint on local buckling of a flat stiffener is defined by means of the limiting slenderness ratio according to Eurocode 3 (EC 3) [4.23]

$$\frac{h_s}{t_s} \leq \frac{1}{\beta_s} = 14 \sqrt{\frac{235}{f_y}} \quad (4.5.9)$$

The optimization procedure is carried out by using the software for *the feasible sequential quadratic programming FSQP method* developed by Zhou and Tits [4.15] and for *the Rosenbrock's hillclimb method*. Rounded values are computed by a complementary special program.

Table 4.5.2. Optimal versions of a uniaxially compressed longitudinally stiffened plate, double fillet welds carried out by different welding methods, dimensions in mm

Welding method	k_f/k_m	t_f	h_s	t_s	φ	A (mm ²)	K/k_m (kg)
SMAW	0.00	9.7	202	14.4	15.0	84584	2656
	0.10	11.7	204	17.4	11.7	90372	3572
	0.18	13.8	217	15.6	9.5	89923	3688
	0.20	17.1	225	17.9	7.0	99632	4057
	0.50	19.3	232	16.6	5.7	103068	4867
	1.00	20.0	233	16.7	5.4	104956	6425
	1.50	20.0	234	16.7	5.3	104730	7919
GMAW-C	0.0	9.7	202	14.4	15.0	84584	2656
	0.3	12.0	206	17.6	11.1	102069	3754
	0.5	15.4	222	15.9	8.0	93118	3823
	1.0	17.3	228	16.4	6.7	97615	4661
	1.5	20.0	234	16.7	5.3	104730	5262
SAW	0.0	9.7	202	14.4	15.0	84584	2656
	0.5	12.0	212	16.3	11.2	89067	3727
	1.0	15.2	222	15.9	8.2	92730	4194
	1.5	17.3	228	16.3	6.7	97602	4737

The ranges of unknowns are taken as follows (in mm): $t_f = 6 - 20$, $h_s = 84 - 280$, $t_s = 6 - 25$, $\varphi = 4 - 15$.

The computational results are summarized in Tables 4.5.2 and 4.5.3.

Table 4.5.3. Rounded values of those given in Table 4.5.2.

Welding method	k_f/k_m	t_f	h_s	t_s	φ	A (mm ²)	K/k_m (kg)
SMAW	0.00	10	200	15	15	88125	2732
	0.10	12	210	15	12	95880	3332
	0.18	14	215	16	10	94000	3887
	0.20	17	225	17	7	98770	3926
	0.50	19	230	17	6	107970	5049
	1.00	19	230	17	6	107970	6856
	1.50	19	230	17	6	107970	8664
GMAW-C	0.0	10	200	15	15	88125	2732
	0.3	14	215	16	10	94000	3609
	0.5	16	220	16	8	98880	3904
	1.0	17	225	17	7	102970	4879
	1.5	19	230	17	6	107970	5553
SAW	0.0	10	200	15	15	88125	2732
	0.5	12	210	15	12	95880	3611
	1.0	16	220	16	8	98880	4270
	1.5	17	225	17	7	102970	4913

It can be seen that the minimum weight design ($k_f = 0$) results in much more stiffeners than the minimum cost design. The optimal plate dimensions depend on cost factors k_f/k_m and C_2 , so the results illustrate the effect of the welding technology on the structure and costs. It should be noted that, in the case of SMAW, the φ_{opt} values are very sensitive to k_f/k_m , so in Tables 4.5.2 - 4.5.3 more k_f/k_m -values are treated.

For $k_f/k_m = 1.5$ the cost savings achieved by using SAW instead of SMAW or GMAW-C are $100 (7919 - 4737) / 7919 = 40\%$ and $100 (5262 - 4737) / 5262 = 10\%$.

In the case of SMAW and $k_f/k_m = 1.5$ the material cost component is $\rho LA = 3289$ kg, so the fabrication cost represents $100 (7919 - 3289) / 7919 = 58\%$ of the whole cost, this significant part of costs affects the dimensions and the economy of stiffened plates.

4.5.4 CONCLUSIONS

- a) Cost functions are formulated by means of the COSTCOMP software for longitudinal fillet welds carried out with manual SMAW, semi-automatic GMAW-C and automatic SAW method in downhand position.
- b) Using these cost functions the optimal dimensions of a stiffened plate are computed which minimize the total cost and fulfil the design constraints on overall and local buckling.
- c) The comparison of optimal solutions shows that significant cost savings may be achieved by using SAW instead of SMAW or GMAW-C.
- d) Numerical computations show that the optimal dimensions of a stiffened plate depend on the applied welding method and illustrate the necessity of cooperation between designers and fabricators.
- e) Comparison of optimal solutions for minimum weight ($k_f/k_m = 0$) and minimum cost shows that the fabrication cost affects significantly the optimal dimensions, therefore the consideration of the total cost function results in more economic structural versions.

4.6 OPTIMUM DESIGN OF TUBULAR TRUSSES

4.6.1 INTRODUCTION

Modern structures should be safe and economic. The safety is achieved by using stability constraints which describe the behaviour of structures realistically. The economy can be realized by using optimum design to minimize the cost or weight of the structure.

Authors dealing with the optimum design of metal structures make in some cases simplifications to solve the problems easier. E.g. in the optimization of trusses they neglect the overall buckling of compressed members or use too simple stability constraints such as the Euler buckling curve.

It is well known that the Euler buckling curve neglects the very important effect of initial crookedness and residual stresses caused by fabrication processes (welding, cold-forming). These effects can be described only by a more complicated mathematical form. It will be shown in the present paper that the use of the Euler buckling curve causes unsafe design which is not permissible.

Furthermore, the suitable optimum design procedure will be described using all stability constraints necessary for safe design. The case of welded thin-walled tubular trusses is selected for this purpose, in which not only the constraints on overall buckling, but also the constraints on local buckling of plate elements should be considered. The consideration of all important constraints will be illustrated by a numerical example of a simple tubular truss welded from CHS rods.

4.6.2 UNSAFE DESIGN USING THE EULER BUCKLING CURVE

Authors dealing with the optimum design of tubular trusses have neglected the overall buckling of compression members prescribing constant permissible stresses for tension and compression rods (e.g. Khot and Berke [4.24]), or the overall buckling is considered by the Euler buckling formula (e.g. Vanderplaats and Moses [4.25], Saka [4.26], Amir and Hasegawa [4.27])

$$\sigma_E = \pi^2 E / \lambda^2; \quad \lambda = KL / r; \quad r = \sqrt{I_x / A} \quad (4.6.1)$$

where E is the elastic modulus, λ is the slenderness, K is the end restraint factor (for pinned ends $K = 1$), I_x is the moment of inertia, A is the cross-sectional area, r is the radius of gyration.

For CHS, using the notation $\delta = D / t = (d - t) / t$, where D is the mean diameter and d is the outside diameter, t is the thickness, the following formulae are valid

$$I_x = \frac{\pi D^3 t}{8} = \frac{\pi D^4}{8\delta}; \quad A = \frac{\pi D^2}{\delta}; \quad r = \frac{D}{\sqrt{\delta}} = a\sqrt{A}; \quad a = \sqrt{\frac{\delta}{8\pi}} \quad (4.6.2)$$

$$\text{Thus, } \sigma_E = \frac{\pi EA}{8K^2 L^2} \delta \quad (4.6.3)$$

It can be seen that the local slenderness δ plays an important role in the buckling strength, therefore the selection of the limiting value δ_L influences the optimum design significantly. The first author has verified [4.28] that the local buckling constraint is active in the optimum design of a concentrically compressed CHS strut. E.g. Vanderplaats and Moses [4.25] have selected for steel tubes the value of $\delta_L = 10$, and this value has been used also by Saka [4.26] and Amir and Hasegawa [4.27] (note that in Amir and Hasegawa [4.27] in Eq.(4.6.3) the erroneous value of 3 is printed instead of 8). Since in the EC 3 $\delta_L = 70 \cdot 235 / f_y$, is given for Class 2 sections to be used in tubular trusses, i.e. 70 for a steel of yield stress $f_y = 235$ MPa and 50 for $f_y = 355$ MPa, the value of 10 is incorrect and leads to uneconomic solutions.

In the contrary, the use of the Euler formula leads to unsafe solutions, since it does not take into account the initial crookedness and residual stresses. In [4.29] the AISC buckling curve has been used. Farkas and Jármai [4.30] have applied the EC 3 buckling formulae and have shown that the optimal slope angle of a roof truss depends on the cross-section type of compression members and the use of CHS is much more economic than that of double angle profile.

In the following we compare the cross-sectional areas of a CHS compressed strut calculated from the Euler curve and from the EC 3 buckling formula. In the calculations the values of $f_y = 355$ MPa, $a_L = \sqrt{50 / (8\pi)} = 1.4105$ and $K = 1$ are used. Using Eq. (4.6.2) the slenderness can be expressed by A as follows.

$$\lambda^2 = \frac{L^2}{r^2} = \frac{L^2}{a^2 A} = \frac{10^4}{a^2} \cdot \frac{1}{10^4 A / L^2} = \frac{5027}{10^4 A / L^2} \quad (4.6.4)$$

The overall buckling constraint, using the Euler formula, is

$$\frac{N}{A} \leq \chi f_y ; \quad \chi = \frac{1}{\bar{\lambda}^2} \quad \text{for } \bar{\lambda} \geq 1 \quad (4.6.5)$$

$$\chi = 1 \quad \text{for } \bar{\lambda} \leq 1$$

$$\text{where } \bar{\lambda} = \lambda / \lambda_E; \quad \lambda_E = \pi \sqrt{E / f_y} = 76.4091 \quad (4.6.6)$$

$$\text{From } \frac{10^4 N / L^2}{10^4 A / L^2} \leq \frac{f_y}{\bar{\lambda}^2} = \frac{f_y \lambda_E^2}{\lambda^2} \quad (4.6.7)$$

$$\text{using Eq. (4.6.4) one obtains } \frac{10^4 A}{L^2} = \frac{1}{76.4091} \sqrt{\frac{5027}{355}} \sqrt{\frac{10^4 N}{L^2}} = 0.049247 \sqrt{\frac{10^4 N}{L^2}} \quad (4.6.8)$$

$$\text{valid for } \lambda \geq \lambda_E. \text{ For } \lambda \leq \lambda_E \text{ taking } \chi = 1 \text{ in Eq. (4.6.5) we get } \frac{10^4 A}{L^2} \geq \frac{10^4 N}{L^2 f_y} \quad (4.6.9)$$

According to the EC 3 the overall buckling constraint is

$$\frac{N}{A} \leq \frac{\chi f_y}{\gamma_{M1}}; \quad \gamma_{M1} = 1.1; \quad \frac{1}{\chi} = \phi + \sqrt{\phi^2 - \bar{\lambda}^2}$$

$$\phi = 0.5 \left[1 + 0.34 (\bar{\lambda} - 0.2) + \bar{\lambda}^2 \right] \quad (4.6.10)$$

Introducing the symbols $c_o = 100K/\lambda_E$, $x = 10^4 N/L^2$ and $y = 10^4 A/L^2$, where L [mm] is the strut length, A [mm²] is the required cross-sectional area, N is the factored compressive force in [N], Eq. (4.6.10) can be written as

$$\frac{\gamma_{M1} x}{f_y} \leq \frac{y}{\phi + \sqrt{\phi^2 - \frac{c_o^2}{a^2 y}}}$$

$$\phi = 0.5 \left[1 + 0.34 \left(\frac{c_o}{a \sqrt{y}} - 0.2 \right) + \frac{c_o^2}{a^2 y} \right]; \quad \lambda = \frac{100K}{a \sqrt{y}} \quad (4.6.11)$$

Table 4.6.1. Required $10^4 A/L^2$ -values for some $10^4 N/L^2$ -values in the case of a compressed CHS strut, $f_y = 355$ MPa, $K=1$

$10^4 N / L^2 \left[\frac{N}{mm^2} \right]$		10	100	305.7	1000	10000
$\frac{10^4 A}{L^2}$	Euler	0.1557	0.4925	0.8610	2.8169	28.17
	Eurocode	0.1766	0.6273	1.3171	3.4975	30.60
	difference %	12	21	35	19	8
	λ	168	89	66	38	13

A computer method is used to calculate y for a given x . Results are summarized in Table 4.6.1. It can be seen that the results obtained by the Euler formula are unsafe by 19-35% in the range of $\lambda = 38 - 89$, so the Euler formula gives incorrect solutions.

4.6.3 NUMERICAL EXAMPLE OF A TUBULAR TRUSS

In order to illustrate the role of stability constraints we select a simple planar, statically determinate, K-type truss with parallel chords and gap joints, welded from CHS rods (Fig. 4.6.1). In the optimum design the optimal distance of chords h is sought which minimizes the total volume of the structure and the dimensions of rods fulfil the design constraints. The structural members are divided to 4 groups of equal cross-section as follows: 1 - lower chord, 2 - upper chord, 3 - compression braces, 4 - tension braces.

According to DIN 2448 and DIN 2458 [4.31] the available CHS have the following dimensions (discrete values):

$d = 133, 139.7, 152.4, 159, 168.3, 177.8, 193.7, 219.1, 244.5, 273, 298.5, 323.9$

$t = 2.9, 3.2, 3.6, 4, 4.5, 5, 5.6, 6.3, 7.1, 8, 8.8, 10.$

All members are made from steel Fe 510 with ultimate strength $f_u = 510$ MPa and yield stress $f_y = 355$ MPa.

The load is shown in Fig. 4.6.1, the factored value of the static forces is $F = 200$ kN. Calculate the required cross-sections for various values of $\omega = h/a_o$ to select the ω_{opt} which minimizes the total volume V . The variables are as follows: d_i and t_i ($i=1,2,3,4$). The objective function is expressed as

$$\frac{V}{2\pi a_o} = 5(d_1 - t_1)t_1 + 4(d_2 - t_2)t_2 + 3\sqrt{\omega^2 + 1}(d_3 - t_3)t_3 + 2\sqrt{\omega^2 + 1}(d_4 - t_4)t_4 \quad (4.6.12)$$

The constraints are as follows.

Local buckling constraints for all sections according to Wardenier et al. [4.32] are

$$d_i / t_i \leq 50 \quad (4.6.13)$$

Stress constraint for tension members are

$$\frac{S_{1max}}{\pi(d_1 - t_1)t_1} \leq \frac{f_y}{\gamma_{Mo}}; \quad S_{1max} = \frac{6.5F}{\omega}; \quad \gamma_{Mo} = 1.1 \quad (4.6.14)$$

$$\frac{S_{4max}}{\pi(d_4 - t_4)t_4} \leq \frac{f_y}{\gamma_{Mo}}; \quad S_{4max} = \frac{1.5F}{\omega} \sqrt{\omega^2 + 1} \quad (4.6.15)$$

Overall buckling constraints for compression members according to EC 3. are as follows

$$\text{Upper chord: } \frac{S_{2max}}{\pi(d_2 - t_2)t_2} \leq \frac{\chi_2 f_y}{\gamma_{M1}}; \quad S_{2max} = \frac{6F}{\omega}; \quad \gamma_{M1} = 1.1 \quad (4.6.16)$$

$$\chi_2 = \frac{1}{\phi_2 + \sqrt{\phi_2^2 - \bar{\lambda}_2^2}}; \quad \phi_2 = 0.5 \left[1 + 0.34(\bar{\lambda}_2 - 0.2) + \bar{\lambda}_2^2 \right]$$

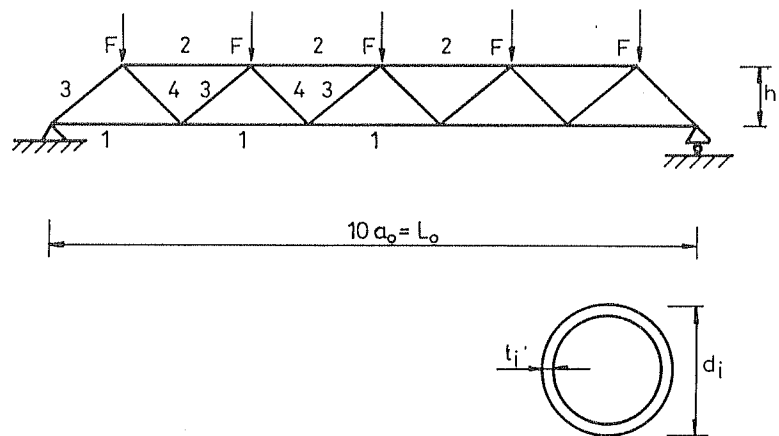


Fig.4.6.1. Planar truss with parallel chords. The numbering relates to groups of members of equal cross-section

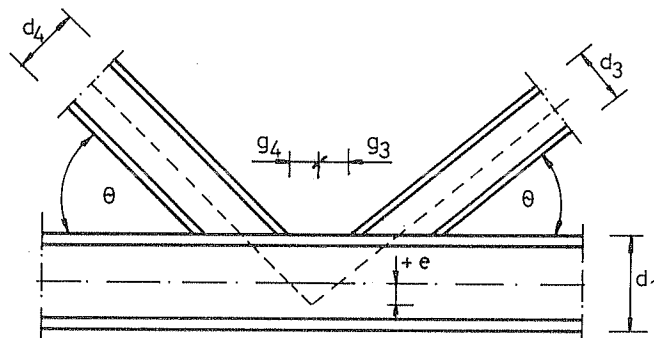


Fig.4.6.2. K-type gap joint with eccentricity e

$$\bar{\lambda}_2 = \frac{\lambda_2}{\lambda_E} = \frac{K_2 L_2}{\lambda_E r_2} = \frac{0.9 * 2a_o \sqrt{8}}{\lambda_E (d_2 - t_2)}.$$

With $E = 2.1 \cdot 10^5$ MPa and $f_y = 355$ MPa $\lambda_E = \pi \sqrt{E / f_y} = 76.4091$.

$K_2 = 0.9$ is the end restraint factor according to Rondal et al. [4.33], $r_2 = (d_2 - t_2) / \sqrt{8}$ is the radius of gyration.

Compression braces:

$$\frac{S_{3max}}{\pi(d_3 - t_3)t_3} \leq \frac{\chi_3 f_y}{\gamma_{M1}}; \quad S_{3max} = \frac{2.5F}{\omega} \sqrt{\omega^2 + 1} \quad (4.6.17)$$

$$\chi_3 = \frac{1}{\phi_3 + \sqrt{\phi_3^2 - \bar{\lambda}_3^2}}; \quad \phi_3 = 0.5 \left[1 + 0.34(\bar{\lambda}_3 - 0.2) + \bar{\lambda}_3^2 \right]$$

$$\bar{\lambda}_3 = \frac{\lambda_3}{\lambda_E} = \frac{K_3 L_3}{\lambda_E r_3} = \frac{0.75a_o \sqrt{\omega^2 + 1} \sqrt{8}}{\lambda_E (d_3 - t_3)}$$

In order to ease the fabrication the diameter of braces should be smaller than those of chords:

$$d_3 = 0.92d_1; \quad d_3 \leq 0.92d_2; \quad d_4 \leq 0.92d_1; \quad d_4 \leq 0.92d_2 \quad (4.6.18)$$

Prescription for the joint eccentricity to avoid too large additional bending moment in the vicinity of nodes is as follows (Fig. 4.6.2):

$$e \leq 0.25d_1; \quad e \leq 0.25d_2 \quad (4.6.19)$$

The eccentricity can be expressed by d_i , angle θ and gap parts g_3 and g_4 as follows:

$$\tan \theta = \frac{e + d_1 / 2}{g_3 + d_3 / (2 \sin \theta)} \quad \text{or} \quad \tan \theta = \frac{e + d_1 / 2}{g_4 + d_4 / (2 \sin \theta)} \quad (4.6.20)$$

Assuming that

$$g_3 = g_4 = 0.05 d_1 \quad \text{or} \quad 0.05 d_2 \quad (4.6.21)$$

the geometry constraints can be given by: $\frac{d_3}{2} \sqrt{\omega^2 + 1} + d_1 (0.05\omega - 0.75) \leq 0 \quad (4.6.22)$

and

$$\frac{d_3}{2} \sqrt{\omega^2 + 1} + d_2 (0.05\omega - 0.75) \leq 0 \quad (4.6.23)$$

Constraint on static strength of welded joints between chords and braces according to EC 3 is

$$\sqrt{\sigma_{\perp}^2 + 3(\tau_{\perp}^2 + \tau_{\parallel}^2)} \leq f_u / (\beta_w \gamma_{Mw}) \quad (4.6.24)$$

$$f_u = 510 \text{ MPa}, \quad \beta_w = 0.9, \quad \gamma_{Mw} = 1.25.$$

From the force S in a brace the following stress components arise in

$$\text{welds: } \sigma_{\perp} = \tau_{\perp} = \frac{S \sin \theta}{\pi d a_w} \cdot \frac{\sqrt{2}}{2}; \quad \tau_{\parallel} = \frac{S \cos \theta}{\pi d a_w} \quad (4.6.25)$$

where a_w is the fillet weld dimension. Substituting Eq. (4.6.25) into Eq. (4.6.24) we get

$$\frac{S}{\pi d a_w} \sqrt{\frac{2\omega^2 + 3}{\omega^2 + 1}} \leq 453 \text{ MPa} \quad (4.6.26)$$

For the maximal value of a_w the corresponding brace thickness can be taken. This constraint should be fulfilled for S_3 and S_4 .

For the node strength the following constraints should be fulfilled (Wardenier et al. [4.32]).

Constraints on chord plastification.

In the joint of rods 1 and 3:

$$S_{3max} \leq S_{31}^* = \frac{f_y t_1^2}{\sin \theta} \left(1.8 + 10.2 \frac{d_3}{d_1} \right) f_1(\gamma_1, g_1') \quad (4.6.27)$$

$$f_1(\gamma_1, g_1') = \gamma_1^{0.2} \left[1 + \frac{0.024 \gamma_1^{1.2}}{\exp(0.5 g_1' - 1.33) + 1} \right]; \quad \gamma_1 = \frac{d_1}{2t_1}$$

$$g_1' = g_1 / t_1; \text{ we assume that } g_1 = g_3 + g_4 = 0.1 d_1$$

Constraints on chord plastification for joints of rods 1 - 4, 2 - 3 and 2 - 4 can be formulated similarly to Eq. (4.6.27), therefore these constraints are not detailed here.

Constraints on punching shear.

In the joint of rods 2 and 3:

$$S_{3max} \leq \frac{f_y}{\sqrt{3}} t_2 \pi d_3 \frac{1 + \sin \theta}{2 \sin^2 \theta} \quad (4.6.28)$$

Note that the constraint on punching shear was in our calculations always passive, so it is not necessary to investigate it for other joints.

For the computations the Rosenbrock's hillclimb mathematical programming method has been used treating the unknowns as continuous variables. After the determination of the optimal dimensions the discrete optima have been found by using an additional search. The results are summarized in Table 4.6.2.

Table 4.6.2. Optimal discrete dimensions [mm] and $V/(2\pi a_0)$ - values [mm²] for various $\omega = h/a_0$ - values.

$\omega = h/a_0$	0.8	0.9	1.0	1.1	1.2	1.3	1.4
d_1/t_1	244.5/8	244.5/8	244.5/8	219.1/8	273/8	273/8	298.5/8.8
d_2/t_2	273/8	244.5/8	244.5/8	219.1/8.8	273/8	273/8	298.5/8.8
d_3/t_3	219.1/4.5	219.1/4.5	219.1/4.5	193.7/4.5	219.1/4.5	219.1/4.5	293.7/4.5
d_4/t_4	159/3.6	152.4/3.6	152.4/3.2	152.4/3.2	139.7/3.2	139.7/3.2	139.7/2.9
$V/(2\pi a_0)$	23083	22367	22475	21063	24970	25264	28704

The optimal value is $\omega = 1.1$, the difference between the best and worst solution in the range of $\omega = 0.8 - 1.4$ is $100/(28704 - 21063)/21063 = 36\%$. The checks of constraints are summarized in Table 4.6.3.

It can be seen that the overall buckling constraint is always active, the local buckling constraint is passive only for chord 2, since for thickness t_2 the chord plastification is governing. Thus, it can be stated that the effect of stability constraints in the optimum design of tubular trusses is significant.

Table 4.6.3. Check of the constraints for the optimal solution $\omega = 1.1$

Constraint	Dimension	Eq. (4.7..)	1	2	Rod 3	4	Remarks
Local buckling	-	(13)	27<50	25<50	43<50	48<50	active for rods 3, 4
Tensile stress	MPa	(14) (15)	223<323	-	-	270<323	near active for rod 4
Overall buckling	MPa	(16) (17)	-	188<204	240<261	-	active for rods 2, 3
Fabrication	mm	(18)	-	-	194<202	152<202	active for rod 3
Eccentricity	mm	(22) (23)	-	-	-8.32	-	near active for rods 1,2,3
Weld strength	MPa	(26)	-	-	368<453	414<453	near active for rod 4
Chord plastification	kN	(27)	-	-	642<713	405<586	active for rods 3-1
Punching shear	kN	(28)	-	-	642<1744	-	passive

4.6.4 CONCLUSIONS

It is shown that the use of the Euler buckling curve instead of the EC 3 overall buckling formula causes 19 - 35% error in the unsafe side in the most important slenderness range of 38 - 89, so it should not be used in the optimization of tubular trusses. The application of limiting tube local slenderness $d/t = 10$ instead of 50 leads to uneconomic solutions. The significant role of the stability constraints in the optimum design of tubular trusses is illustrated by a numerical example. In this optimum design procedure the dimensions of CHS truss members and the optimal distance of chords are determined which give the minimum volume (weight) of the structure and fulfil the design constraints. The constraints relate to the overall buckling of compression members, to the joint eccentricity and static strength of joints. For the final optimal version realistic available discrete tube dimensions are determined.

4.7 SAVINGS IN WEIGHT BY USING CHS OR SHS INSTEAD OF ANGLES IN COMPRESSED STRUTS AND TRUSSES

4.7.1 INTRODUCTION

Some authors dealing with the optimum design of trusses (e.g. Saka [4.34], Koumouis [4.35]) use the conventional rolled angle profiles. The aim of the present paper is to show the advantages of circular or square hollow sections (CHS or SHS) by calculating the weight savings in the case of compressed struts and trusses.

The main advantages of CHS or SHS over angle sections are as follows. 1) the overall buckling strength is higher. This is expressed e.g. in EC 3 (1992) prescribing the buckling curve (b) for CHS and SHS and curve (c) for angles. 2) the radius of gyration (r) in function of the cross-sectional area (A) is much higher than that for double angle profiles. 3) the effective buckling length of chords and braces in trusses is smaller than that of angle profiles.

Trusses constructed from angles have several other disadvantages such as difficulties in manufacturing of nodes with gusset plates or the need of connecting the pairs of angles in prescribed distances. It should be noted that our investigations relate to trusses of larger roofs or smaller bridges and not to columns or towers in which single angle profiles can be advantageously used without gusset plates.

4.7.2 DESIGN OF CENTRALLY COMPRESSED STRUTS

The radius of gyration (r) can be expressed by the cross-sectional area (A) as follows. For CHS and SHS this relationship can be exactly expressed using the local slenderness

$$\delta_c = D/t \text{ and } \delta_s = b/t$$

where D and b are the mean diameter and mean width, t is the thickness (Fig. 4.7.1).

Limiting values for δ_c and δ_s are given for instance by EC 3 for CHS $\delta_{cl} = 70 * 235 / f_y$

where f_y is the yield stress, so for $f_y = 235$ and 355 MPa $\delta_{cl} = 70$ and 50 , respectively.

Note that, according to CIDECT (Wardenier et al. [4.32]), for both steel grades $\delta_{cl} = 50$ is given. For SHS, according to CIDECT (Packer et al. [4.36]),

$$\delta_{sl} = 1.25 \sqrt{E / f_y}$$

thus, for steels of $f_y = 235$ and 355 MPa, $\delta_{sl} = 35$ and 30 , resp. The formulae and values of a_c and a_s are summarized in Table 4.7.1.

For hot rolled equal leg double-angle sections an approximate a_d value can be obtained using r and A values of standard sections according to ISO 657-1 (1989) or DIN 1028 (1976). The calculations result in 0.6938 for single angles and

$$a_d = 0.6938 / \sqrt{2} = 0.49, \quad r = 0.49\sqrt{A}$$

Table 4.7.1. The radius of gyration expressed by cross-sectional area for CHS and SHS

	CHS	SHS
A	$\pi D^2 / \delta_c$	$4b^2 / \delta_s$
I_x	$\pi D^4 / (8\delta_c)$	$b^4 / (24\delta_s)$
$r = \sqrt{I_x / A} = a\sqrt{A}$	$a_c = \sqrt{\delta_c / (8\pi)}$	$a_s = \sqrt{\delta_s / 24}$
$\delta_L (f_y = 235 \text{ MPa})$	$\delta_{cL} = 70$	$\delta_{sL} = 35$
$\delta_L (f_y = 355 \text{ MPa})$	$\delta_{cL} = 50$	$\delta_{sL} = 30$
$a (f_y = 235 \text{ MPa})$	$a_{cL} = 1.6689$	$a_{sL} = 1.2076$
$a (f_y = 355 \text{ MPa})$	$a_{cL} = 1.4105$	$a_{sL} = 1.1180$

for double-angle profiles. It can be seen that a_d is much smaller than a_{cL} and a_{sL} .

In the optimum design of a concentrically compressed strut the cross-sectional area should be minimized considering the overall and local buckling constraints:

$A \rightarrow \min.$

The overall buckling constraint is defined according to the EC 3 as follows.

$$\begin{aligned} N / A &\leq \chi f_y; \quad 1 / \chi = \phi + \sqrt{\phi^2 - \bar{\lambda}^2} \\ \bar{\lambda} &= \lambda / \lambda_E = KL / (r \lambda_E); \quad \lambda_E = \pi \sqrt{E / f_y} \\ \phi &= 0.5 \left[1 + \alpha (\bar{\lambda} - 0.2) + \bar{\lambda}^2 \right] \end{aligned} \quad (4.7.1)$$

where $\alpha = 0.34$ for CHS and SHS, $\alpha = 0.49$ for double angle sections. K is the end restraint factor, for double angles $K = 1$, for CHS and SHS in trusses, according to CIDECT (Rondal et al. [4.33]), for chords $K = 0.9$, for braces $K = 0.75$. For $E = 2.1 \times 10^5$ MPa and $f_y = 235$ MPa $\lambda_E = 93.91$.

The local buckling constraint is

$$\delta \leq \delta_L \quad (4.7.2)$$

Treating Eq. (4.7.2) as equality (active constraint) the two unknown sizes of CHS or SHS (D , t) or (b , t) can be calculated.

In the optimum design of tubular trusses these sizes should be treated separately, since the strength and geometric limitations for truss nodes rely on these unknowns [4.16]. Instead of these sizes we use here the relationship $r = a\sqrt{A}$, since this method is suitable for angle sections.

Using this relationship, A will be the sole unknown in the overall buckling constraint.

Introducing the symbols

$$c_o = 100K / \lambda_E, \quad x = 10^4 N / L^2, \quad y = 10^4 A / L^2$$

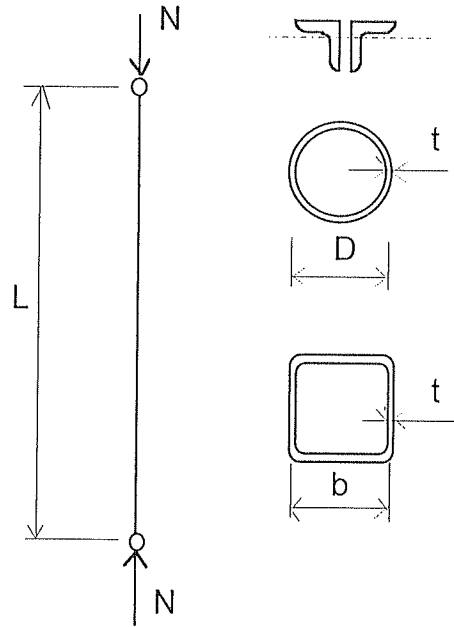


Fig. 4.7.1 Compressed strut of CHS, SHS and double-angle section

where L is the strut length in [mm], A in [mm²], N is the compressive force in [N], Eq. (4.7.1) can be written as

$$\frac{x}{f_y} \leq \frac{y}{\phi + \sqrt{\phi^2 - \frac{c_o^2}{a^2 y}}} \quad (4.7.3)$$

$$\phi = 0.5 \left[1 + \alpha \left(\frac{c_o}{a \sqrt{y}} - 0.2 \right) + \frac{c_o^2}{a^2 y} \right]$$

Unfortunately, it is impossible to solve Eq. (4.7.3) for y in closed form, therefore a computer method is used to calculate y for given x .

Table 4.7.2 shows the relationships $10^4 N / L^2 - 10^4 A / L^2$ for CHS, SHS and double-angle sections in a double log coordinate system. In the case of CHS and SHS the end restraint factors $K=0.9$ and 0.75 , for double angle sections $K=1$ is considered, so these diagrams can be used for the design of various compression members in trusses.

It can be seen that the cross-sectional area of double-angle profiles is much greater than those of CHS and SHS. The difference or the savings in weight depends on N / L^2 -value or on the strut slenderness λ . The $s = \lambda$ -curve is also given for CHS in the case of $K = 0.9$. The higher the slenderness the larger the weight savings.

Table 4.7.2. Required $10^4 A / L^2$ values and slendernesses $s = \lambda = KL / r$ in function of $10^4 N / L^2$ in double-log coordinate system for CHS and SHS in the case of $K = 0.9$ and 0.75 , resp. and for double-angle section for $K = 1$. Slendernesses are given only for CHS with $K = 0.9$. All values are calculated for yield stress $f_y = 235$ MPa

$10^4 N / L^2$	10	100	1000	10000
CHS-0.9	0.1327	0.559	4.36	40.93
CHS-0.75	0.106	0.469	4.24	40.67
SHS-0.9	0.1792	0.672	4.51	41.4
SHS-0.75	0.1457	0.52	4.32	41.01
Angles 1.0	0.484	1.66	6.79	45.6
Slenderness for CHS-0.9	148	72.1	25.8	8.4

The ratio between the A / L^2 -values for double-angle sections and CHS $K = 0.9$ varies from 3.5 to 1.1 in the range of

$$10^4 N / L^2 = 25 - 10000 \quad (\lambda = 114 - 8).$$

For SHS $K = 0.9$ this ratio varies from 2.7 to 1.1. These numbers illustrate the significant weight savings.

It should be noted that, for design purposes of CHS and SHS struts, the Japanese Road Association (JRA) overall buckling curve (Hasegawa et al. [4.37]) can be used instead of EC 3 curve (b). In this case closed formulae can be given for cross-sectional sizes.

$$N / A \leq \chi f_y$$

$$\begin{aligned} \chi &= 1 & \text{for } 0 \leq \bar{\lambda} \leq 0.2 \\ \chi &= 1.109 - 0.545 \bar{\lambda} & \text{for } 0.2 \leq \bar{\lambda} \leq 1 \\ \chi &= \frac{1}{0.773 + \bar{\lambda}^2} & \text{for } \bar{\lambda} \geq 1 \end{aligned} \quad (4.7.4)$$

Introducing the symbols

$$\mathcal{G}_c = 100D / L \quad \text{and} \quad \mathcal{G}_s = 100b / L$$

and using $\bar{\lambda} = c / \mathcal{G}$ the closed formulae are as follows.

For $0.2\mathcal{G} \leq c \leq \mathcal{G}$

$$\mathcal{G} = 0.24572 c \left[1 + \sqrt{1 + \frac{14.93475\nu}{c^2}} \right] \quad (4.7.5.a)$$

and for

$$\mathcal{G} \leq c$$

$$\mathcal{G} = \left\{ 0.3865\nu \left[1 + \sqrt{1 + \frac{6.69424c^2}{\nu}} \right] \right\}^{1/2} \quad (4.7.5.b)$$

$$\text{for CHS } c_c = \frac{100K\sqrt{8}}{\lambda_E}, \quad v_{CL} = \frac{10^4 N}{L^2} \cdot \frac{\delta_{CL}}{\pi f_y}$$

$$\text{for SHS } c_s = \frac{100K\sqrt{6}}{\lambda_E}; \quad v_{SL} = \frac{10^4 N}{L^2} \cdot \frac{\delta_{SL}}{4f_y}$$

4.7.3 NUMERICAL EXAMPLE OF A TRUSS

The design method described in Section 4.7.2 is applied for compression members of a statically determinate roof truss with non-parallel chords to illustrate the savings in weight in the case of trusses by using CHS or SHS instead of double-angle sections. Consider the truss shown in Fig. 4.7.2. Four different cross-sections (1-4) are designed for each case. To find the optimal truss height (h) or the optimal slope angle of the upper chord, the truss is designed for heights $h=2.5, 3.5, 4.5, 6.0$ and 7.5 m (corresponding slope angles are $(4.76^\circ, 9.46^\circ, 14.04^\circ, 20.56^\circ$ and $26.56^\circ)$).

In the design of CHS and SHS struts, section properties of the ISO/DIS 4019.2 as well as the tables given by Dutta and Würker [4.31] (DIN 2448, DIN 2458, DIN 59411) have been used. The results of the calculations are summarized in Table 4.7.3. and Fig.4.7.2.

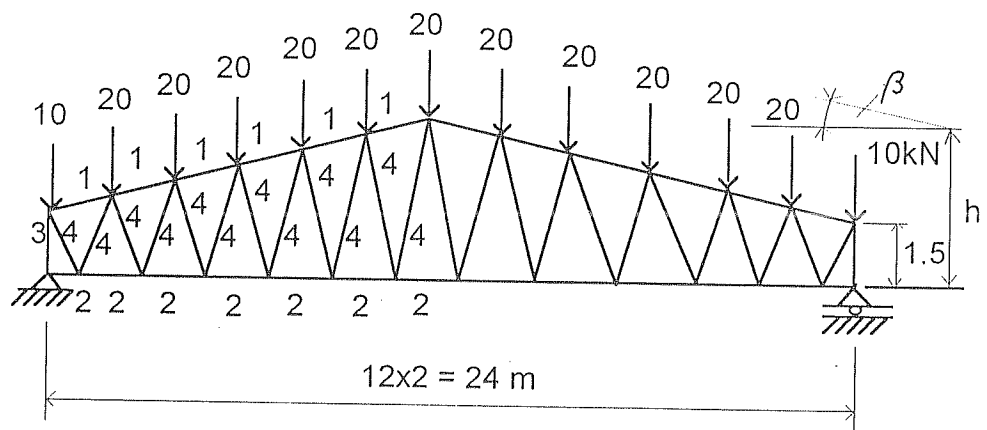


Fig. 4.7.2 Numerical example of a roof truss. 1 - section for upper chord, 2 - section for lower chord, 3 - section for outside columns, 4 - section for braces. The height h varies with the slope angle β of the upper chord.

Table 4.7.3. Total volumes of trusses of various heights

Height h (m)	Slope angle β°	Section	Upper chord 1	Lower chord 2	Outside columns 3	Braces 4	Total volume $10^{-7} \text{ (mm}^3\text{)}$
2.5	4.76	CHS	152.4/2.9	133/3.2	108/2.3	108/2.3	10.72
		SHS	115/3.2	110/3	70/3.2	70/3.2	11.04
		angles	2x80x8	2x50x7	2x50x6	2x70x6	18.14
3.5	9.46	CHS	152.4/2.3	139.7/2.3	101.6/2	101.6/2	9.24
		SHS	115/2.6	80/3.2	70/2.6	70/2.6	9.71
		angles	2x70x7	2x50x5	2x50x6	2x55x6	15.36
4.5	14.04	CHS	139.7/2	127/2	101.6/2	101.6/2	8.95
		SHS	90/3	80/2.6	70/2.6	70/2.6	9.80
		angles	2x65x7	2x45x5	2x50x6	2x60x6	17.18
6.0	20.56	CHS	127/2	101.6/2	101.6/2	88.9/2	8.79
		SHS	90/2.6	90/2	70/2.6	70/2.6	10.45
		angles	2x70x6	2x40x4	2x50x6	2x60x6	18.87
7.5	26.56	CHS	114.3/2	88.9/2.3	101.6/2	88.9/1.8	8.84

It can be seen that the optimal truss height (slope angle) giving the minimal total volume of the structure depends on the cross-sectional shape. In the investigated numerical example the optimal slope angles are as follows:

for double-angle sections

$\beta \cong 10^\circ$, for SHS $\cong 12^\circ$ and for CHS $\cong 20^\circ$.

The savings in weight by using CHS or SHS instead of double-angle sections, according to Table 4.7.2, are 41-53 % or 39-45 %, respectively e.g. $100 (18.14 - 10.72 / 18.14) = 41 \%$ etc.

These differences are larger than the difference between the material costs of CHS, SHS and rolled angles, thus material cost savings can also be achieved.

Note that the sensitivity of the volume functions for CHS and SHS is relatively small, but the difference between the volumes for the heights $h = 2.5$ and the optimal $h_{\text{opt}} = 6$ m (for CHS) is $100 (10.72 - 8.79 / 10.72) = 18 \%$, so, for economic design, it is important to choose the optimal truss slope.

4.7.4 CONCLUSIONS

The overall buckling strength of concentrically compressed CHS and SHS struts is much larger than that of double-angle section struts, therefore significant savings in weight and

material cost can be achieved by using CHS and SHS instead of double-angle sections in compressed struts and trusses.

By using the limiting local slendernesses and the relationships between the radius of gyration and cross-sectional area, design diagrams are given for the calculation of the required cross-sectional area in function of the compressive force and strut length.

The illustrative numerical example of a roof truss, constructed from CHS, SHS or double-angle sections shows that the optimal geometry of the truss depends on the cross-sectional shape of compression members. This conclusion is important, since this aspect has not been pointed out till now in the optimum design of trusses.

4.8 MULTIOBJECTIVE OPTIMUM DESIGN OF WELDED BOX BEAMS

4.8.1 INTRODUCTION

The multiobjective optimization gives designers aspects for selection of the most suitable structural version. Some applications have been treated e.g. in Refs. [4.38, 4.39, 4.40]. Our aim is to show the application of multiobjective optimization technique in an illustrative numerical example of a simple welded box beam.

It has been shown [4.41, 4.18] that the fabrication cost affects the optimal dimensions of welded structures. Therefore we use not only the mass, but also the cost as objective function, which contains the material and fabrication costs. The deflection of a beam is often limited to fulfil the serviceability requirements. E.g. in EC 3, the beam deflection is limited to $L/200$ - $L/500$, where L is the span length. Therefore our aim is to find structural solutions which minimize the maximal deflection.

The design constraints on stresses and local buckling of plate elements are formulated according to EC 3. Several single- and multiobjective optimization methods are used to show their suitability for the solution of the defined nonlinear programming problem.

4.8.2 THE OBJECTIVE FUNCTIONS

The cost function is defined by Eq 4.8.1.

In order to stiffen the box beam against the torsional deformation of the cross-sectional shape, some transversal diaphragms should be used. As shown in Fig.4.8.1, in our example we use 7 diaphragms, so $\kappa = 11$. Note that the mass of these diaphragms is neglected. For the four longitudinal fillet welds we consider the constants $C_2 = 0.4 \cdot 10^{-3}$ and $C_3 = 0.12 \cdot 10^{-3}$ [min/mm^{2.5}], for manual-arc-welded transversal fillet welds connecting the diaphragms to the box beam we use $C_2 = 0.8 \cdot 10^{-3}$ and $C_3 = 0.24 \cdot 10^{-3}$ [min/mm^{2.5}] (see Sections 4.4.2. and 4.5.2).

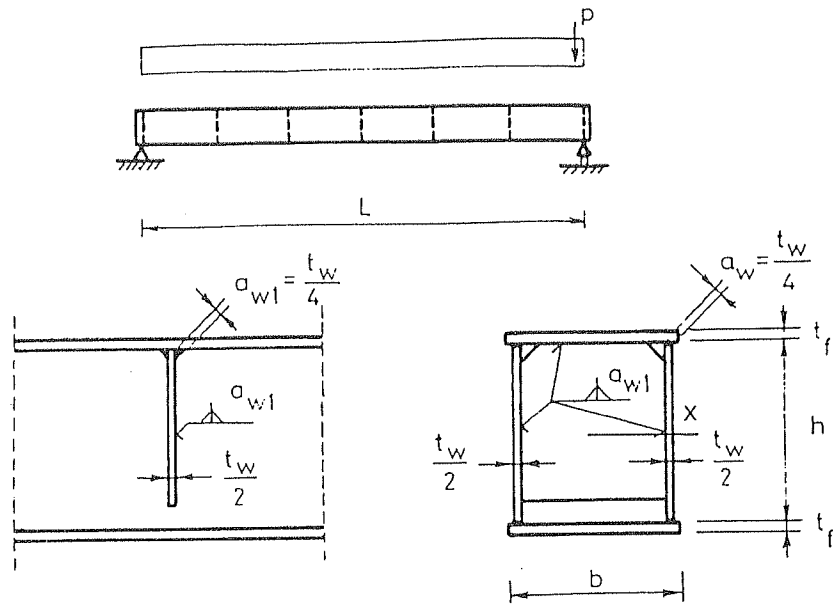


Fig. 4.8.1 Welded box beam with transverse diaphragms

For the difficulty factor we take $\Theta = 2$, so the final formula of the cost function as the first objective function is

$$f_1 = K/k_m(kg) = \rho AL + k_f/k_m * \left[2\sqrt{\rho AL} \sqrt{11} + 0.52 * 10^{-3} * 4L \left(\frac{t_w}{4}\right)^{1.5} + 1.04 * 10^{-3} * 7 * 2(2h + b) \left(\frac{t_w}{4}\right)^{1.5} \right] \quad (4.8.6)$$

Disregarding the fabrication costs, i.e. taking $k_f = 0$, we obtain the mass function as the second objective function

$$f_2 = \rho AL \quad (4.8.7)$$

The third objective function to be minimized is the maximal deflection of the beam due to the uniformly distributed normal static load p_0 neglecting the self mass

$$f_3 = \frac{5p_0 L^4}{384EI_x} \quad (4.8.8)$$

where $E = 2.1 * 10^5$ MPa is the modulus of elasticity for steels,
 I_x is the moment of inertia

$$I_x = \frac{h^3 t_w}{12} + \frac{2bt_f^3}{12} + 2bt_f \left(\frac{h+t_f}{2} \right)^2 \quad (4.8.9)$$

4.8.3 THE DESIGN CONSTRAINTS

The constraint on bending stress, according to EC 3, can be expressed as

$$\sigma_{max} = \frac{\gamma_1 M_{max}}{W_x} \leq \frac{f_y}{\gamma_{M0}} \quad (4.8.10)$$

where the safety factors are as follows

$$\gamma_1 = 1.5 \text{ and } \gamma_{M0} = 1.1$$

The bending moment is

$$M_{max} = \frac{pL^2}{8} \quad (4.8.11)$$

Considering also the self mass

$$p = p_0 + \rho A g \quad (4.8.12)$$

where $g = 9.81 \text{ m/s}^2$ is the gravitational acceleration.

Furthermore, f_y is the yield stress, for steel Fe 360 $f_y = 235$, for steel Fe 510 $f_y = 355 \text{ MPa}$.

The section modulus is

$$W_x = \frac{I_x}{\frac{h}{2} + t_f} \quad (4.8.13)$$

Note that we consider the cross section of class 3 that means that the stress distribution is linear elastic and the yield stress is reached in extreme fibre without any local buckling of plate elements.

Local buckling constraint for compressed upper flange

$$t_f \geq \delta b ; 1/\delta = 42 \varepsilon ; \varepsilon = \sqrt{\frac{235}{\sigma_{max}}} \quad (\sigma_{max} \text{ in MPa}) \quad (4.8.14)$$

and for bent webs

$$t_w/2 \geq \beta h ; 1/\beta = 124 \varepsilon \quad (4.8.15)$$

The shear constraint can be expressed according to EC 3 for $1/\beta = 124\varepsilon$

$$Q_{max} = \frac{\gamma_1 p L}{2} \leq 0.627 * 0.5 Q_b \quad (4.8.16)$$

where

$$Q_b = \frac{h t_w}{\gamma_{M1}} \frac{f_y}{\sqrt{3}}$$

With $\gamma_{M1} = 1.1$ Eq. (4.8.16) takes the form

$$\frac{\gamma_1 p L}{2} \leq 0.1645 h t_w f_y \quad (4.8.17)$$

Since the deflection minimization leads to maximization of the beam dimensions, size constraints should be defined as follows

$$h \leq h_{max}; t_w \leq t_{wmax}; b \leq b_{max}; t_f \leq t_{fmax} \quad (4.8.18)$$

4.8.4 THE OPTIMIZATION PROCEDURE

In the optimization procedure the optimal values of variables h , t_w , b and t_f should be determined which minimize the objective functions and fulfil the design constraints. Note that for the single-objective problem to minimize the mass f_2 , the following approximate formulae can be derived [4.8]

$$h = \sqrt[3]{0.75W_0 / \beta}; t_w/2 = \beta h; b = h \sqrt{\beta / \delta}; t_f = \delta b \quad (4.8.19)$$

where $W_0 = \frac{\gamma_1 M_{max}}{f_y / \gamma_{M0}}$ is the required section modulus.

For the computer-aided optimum design a decision support system has been developed [4.42, 4.43, 4.44] containing five single-objective and seven multiobjective optimization techniques. The single objective optimization methods are as follows: Himmelblau's method of flexible tolerances, Weisman's Direct Random Search method, Rosenbrock's hillclimb method, Complex method of Box and the Davidon-Fletcher-Powell method.

The multiobjective optimization methods are as follows: min-max, weighting min-max, global criterion methods, weighting global criterion, pure weighting; and normalized weighting method.

A multicriteria optimization problem can be formulated as follows :

$$\begin{aligned} &\text{Find } x \text{ such that} \\ &f(x^*) = \text{opt } f(x), \\ &\text{such that} \\ &g_j(x) \geq 0 \quad j = 1, \dots, m \\ &h_i(x) = 0 \quad i = 1, \dots, q \end{aligned} \quad (4.8.20)$$

where x is the vector of decision variables defined in n -dimensional Euclidean space and $f_k(x)$ is a vector function defined in r -dimensional Euclidean space. $g_j(x)$ and $h_i(x)$ are inequality and equality constraints.

The solutions of this problem are the Pareto optima. The definition of this optimum is based upon the intuitive conviction that the point x^* is chosen as the optimal, if no criterion can be improved without worsening at least one other criterion.

We have used the min-max, the weighting min-max, two types of global criterion, weighting global criterion, pure weighting and normalized weighting techniques. They are described in details in [4.38, 4.40].

Description of the methods can be found in [4.45].

4.8.5 THE RESULTS OF A NUMERICAL EXAMPLE

Data: $p_O = 80$ kN/m, $L = 15$ m, $\rho = 7850$ kg/m³, $h_{max} = 1800$, $b_{max} = 1000$, $t_{wmax} = 40$, $t_{fmax} = 40$ mm.

Table 4.8.1 shows the results of the single-objective optimization using three different techniques. The differences between results are very small. All the techniques treat the variables as continuous ones and give unrounded optima. To give plate sizes available in the market, a secondary search is used for finding the discrete optima. The discrete steps for h and b are 50 mm, for thicknesses $t_w/2$ and t_f 1 mm.

Table 4.8.1
Characteristics of beams optimized using different single-objective techniques

Technique		h	t_w (mm)	b	t_f	f_1 (kg)	f_3 (mm)
Flexible tolerance	f_{1min}	1450	22	700	19	9332	19.7
	f_{3min}	1800	32	1000	40	20801	5.1
Direct random search	f_{1min}	1400	22	650	22	9402	20.5
	f_{3min}	1800	32	1000	40	20801	5.1
Hillclimb	f_{1min}	1300	20	550	32	9343	21.9
	f_{3min}	1800	32	1000	40	20801	5.1

In Table 4.8.2 the multiobjective - Pareto - optima are given, obtained using five different techniques, for steel Fe 360 and for the ratio $k_f/k_m = 1.5$. Fig. 4.8.2 shows the results in the coordinate-system $f_1 - f_3$, for steels Fe 360 and Fe 510. The notation f_1^{510} means the optimum of f_1 for steel Fe 510.

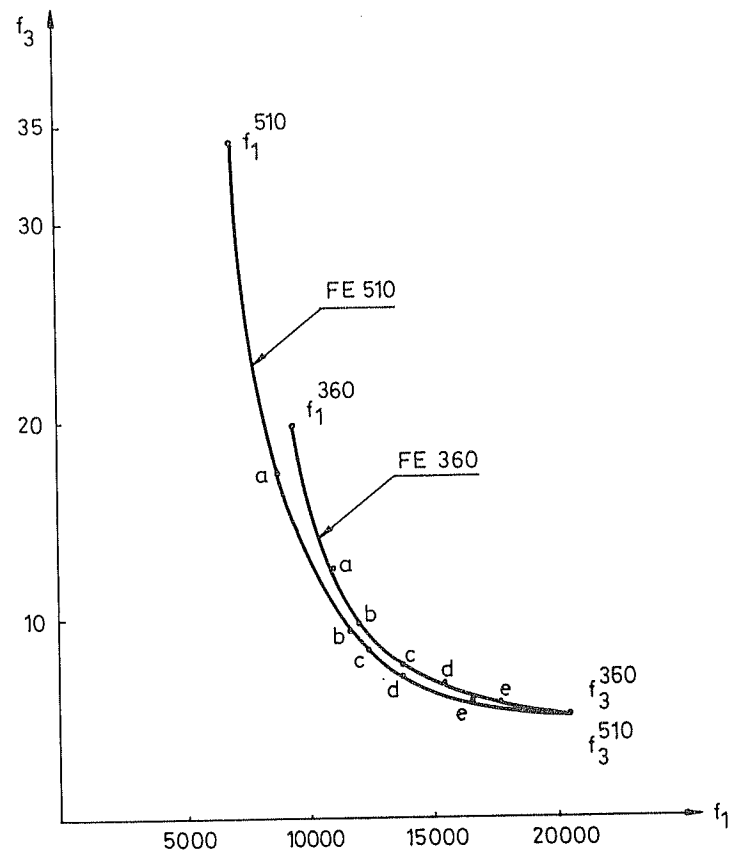
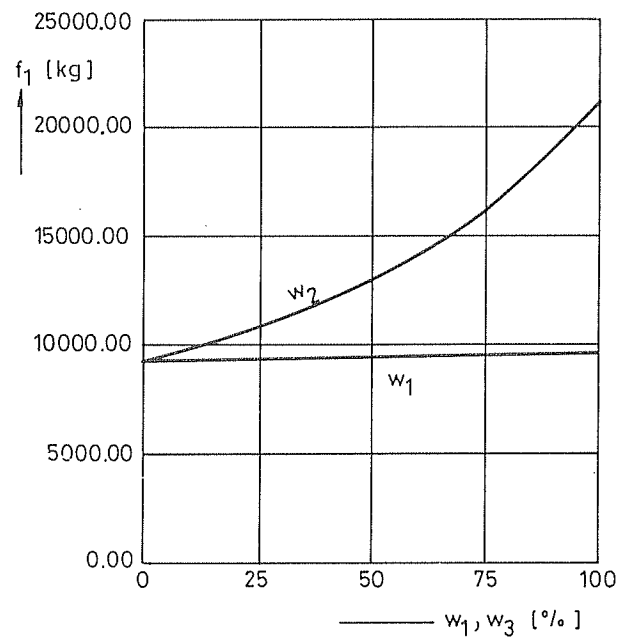
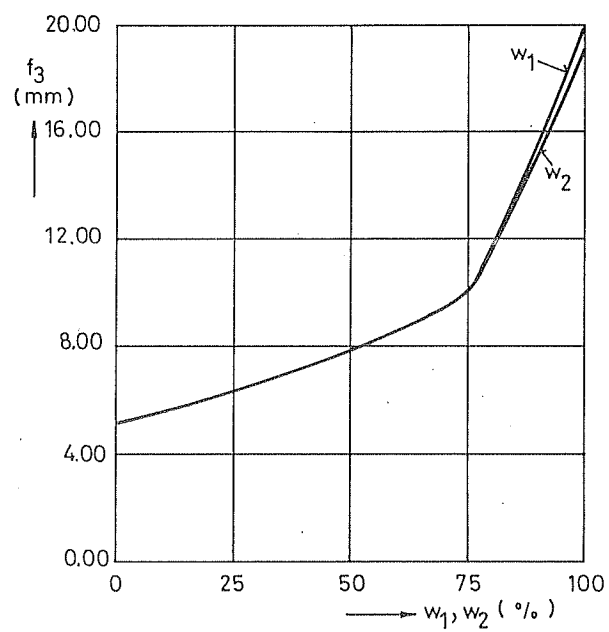


Fig. 4.8.2. Optima in a coordinate-system f_1 - f_3 for various weighting coefficients, for steels Fe 360 and Fe 510, according to the weighting min-max technique. The points relate to the following weighting coefficients: a) $w_1=0.90$, $w_2=0.10$, b) $w_1=0.75$, $w_2=0.25$; c) 0.50/0.50, d) 0.25/0.75 and e) 0.10/0.90

Fig.4.8.3. Effect of weighting coefficients w_2 and w_3 on f_1 Fig.4.8.4. Effect of w_1 and w_2 on f_3

The Pareto-optima for various weighting coefficients of the weighting min-max technique can be seen between the limiting points of the single-objective optima. Note that the points $c/$ are the same also for min-max technique. It can be seen that the single-optimum of the deflection f_3 does not depend on the steel type, i.e. $f_3^{360} = f_3^{510}$.

It can be seen from the Table 4.8.3 that cost savings of 24% may be achieved using Fe 510 instead of Fe 360, but the deflection will be nearly doubled.

Fig. 4.8.3 and 4.8.4 show the effect of the relative importance of an objective function on the value of the other objective function.

Table 4.8.2

Characteristics of beams optimized using different multiobjective optimization methods and various weighting coefficients

Technique	h	t_w (mm)	b	l_f	f_1 (kg)	f_3 (mm)
min-max	1800	20	750	39	13762	7.3
global 1, P=3	1800	20	750	40	13947	7.2
global 2, P=5	1800	20	900	33	13910	7.2
weighting min-max						
w_1/w_3						
0.9/0.1	1750	24	700	18	10834	12.2
0.75/0.25	1800	22	950	20	11974	9.5
0.5/0.5	1800	20	750	39	13762	7.3
0.25/0.75	1800	18	1000	38	15294	6.1
0.1/0.9	1800	24	1000	40	17869	5.5
weighting global						
0.9/0.1	1800	22	950	20	11974	9.5
0.75/0.25	1800	20	900	28	12799	8.2
0.5/0.5	1800	20	950	35	14329	7.0
0.25/0.75	1800	18	950	40	15284	6.1
0.10/0.9	1800	18	1000	40	15786	5.9
normalized weighting						
0.9/0.1	1800	26	500	13	10136	14.0
0.75/0.25	1800	22	950	20	11974	9.5
0.5/0.5	1800	18	950	40	15284	6.1
0.25/0.75	1800	22	950	40	16658	5.9
0.1/0.9	1800	32	1000	40	20801	5.1

Table 4.8.3

Characteristics of optimized beams made of steel Fe 360 and Fe 510

Steel	Technique		h	t_w	b (mm)	t_f	f_1 (kg)	f_3 (mm)
Fe 360	Single-objective	f_{1min}	450	22	700	19	9332	19.7
	optimization	f_{3min}	1800	32	1000	40	20801	5.1
	min-max method		1550	30	750	25	16343	8.8
Fe 510	Single-objective	f_{1min}	1300	20	500	17	7051	34.2
	optimization	f_{3min}	1800	32	1000	40	20301	5.1
	min-max method		1500	24	750	40	14253	10.2

Table 4.8.4 shows the results of the single-objective optimization for Fe 360 and $k_f/k_m = 1.5$ for the three objective functions.

Table 4.8.4

Characteristics of beams optimized using single-objective optimization technique

Objective function	h	t_w (mm)	b	t_f	f_1 (kg)	f_2 (kg)	f_3 (mm)
f_1	1450	22	700	19	9332	6888	19.7
f_2	1500	24	700	16	9577	6876	19.0
f_3	1800	32	1000	40	20801	16202	5.1

4.8.6 CONCLUSIONS

The investigated numerical example illustrates the possibilities given for designers to select the most suitable structural version considering the cost, mass and maximal deflection of a structure.

It can be seen from Table 4.8.4 that the fabrication cost is about 26% of the total cost and therefore does not affect significantly the optima. In other words, the mass and the cost function are only slightly conflicting. Therefore the mass f_2 is not shown in Figures. The effect of fabrication cost is much more significant in the case of a stiffened plate as it has been shown in another study [4.18].

The deflection minimization leads to maximal prescribed sizes and to significant increase of cost and mass. The use of steel Fe 510 instead of Fe 360 results in 24% cost savings without deflection minimisation and no savings considering the deflection minimisation. The multiobjective optimization gives structural versions for selected weighting coefficients according to Table 4.8.2 and Fig. 4.8.2.

4.9 FABRICATION COST CALCULATION AND OPTIMUM DESIGN OF WELDED STEEL SILOS

4.9.1 INTRODUCTION

Silos are used for many engineering purposes. Several structural versions exist for ground or elevated silos, for storage and transportation of different materials such as coal, sand, cement, grains (wheat, peas etc.). Silos may be constructed from steel, aluminium or reinforced concrete. Steel silos can be welded or bolted. Corrugated plate elements are also used (Martens [4.46]).

A transit silo constructed from steel plate elements is investigated in the present paper (Fig.4.9.1). This type consists of the following main structural parts: roof, circular cylindrical bin, transition ringbeam, conical hopper and supporting columns. Our aim is to show the design procedure and fabrication cost calculations of these parts and to give designers aspects for the minimum weight and cost design.

Many articles can be found in the literature dealing with the stress and strength analysis of such silos (e.g. Gaylord [4.47], Trahair et al. [4.48], Teng and Rotter, [4.49]), but the minimum cost design is not treated till now.

The main structural dimensions of a silo shown in Fig.4.9.1 are the height H and radius R of the cylindrical bin welded from horizontal courses of thin plates. For a given stored material, storage capacity of the bin and hopper, for a H/R ratio and H , the R value can be calculated and the structural dimensions of the silo parts can be designed on the basis of stress and buckling strength constraints.

The question of the optimum design is to determine the optimal H/R ratio for which the self weight of the structure and the cost is minimal. To illustrate the behaviour of these objective functions a numerical example is selected and self weight and cost calculations are performed for various H/R ratios.

The slope angle of the hopper is determined by the friction angle of stored material, so it is not varied. The number of columns can be varied, but the maximal number is determined by the required minimal distance between columns to allow the emptying into lorries, and the minimal number is 6, required for the stability against horizontal action of wind and earthquake.

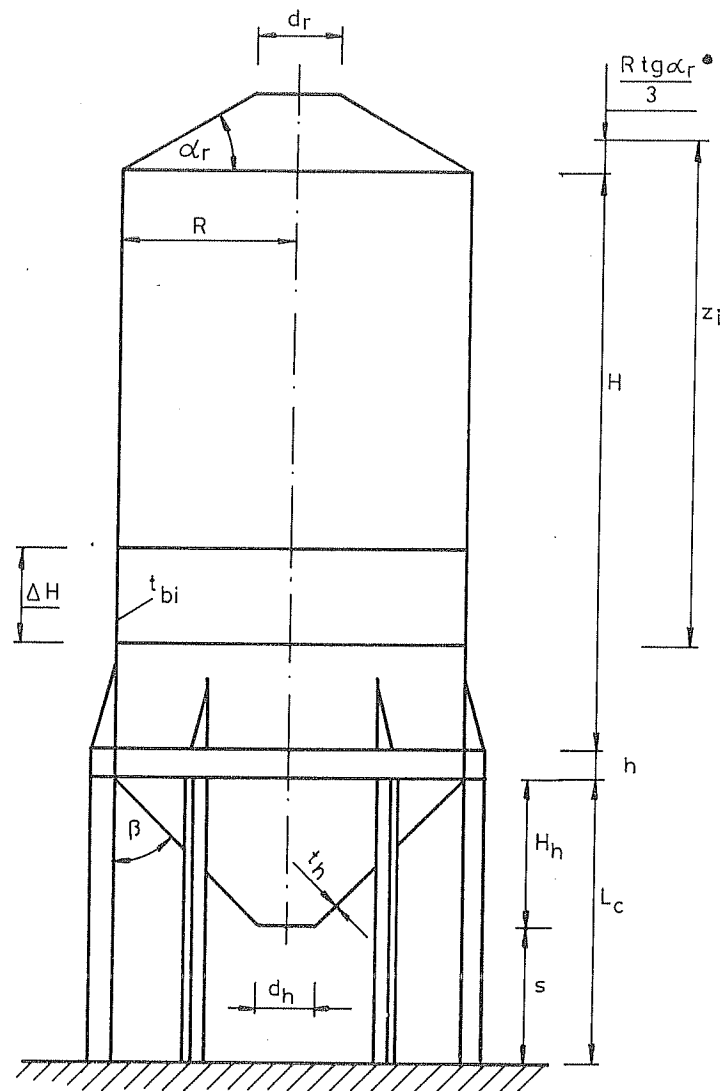


Fig.4.9.1. Main dimensions of a welded steel silo

The design procedure and cost calculations are treated considering the practical ranges of dimensions regarding the numerical example. It should be noted that it is impossible to give general optimum design rules valid for all types of silos and all ranges of dimensions. For other types and dimensions a similar analysis and optimum design should be carried out. Fig. 4.9.1.

4.9.2 THE COST FUNCTION

The objective function is defined according to Section 4.5.2.

The values of $C_2 a_w''$ in Eq. (4.5.3) are given on the basis of the COSTCOMP [4.20] software worked out by the Welding Institute of Netherlands (Bodt [4.21]) for some weld types and welding methods in Table 4.9.1. (Table 4.5.1. is complemented with another values needed for silos).

Table 4.9.1. Welding times T_2 (min/mm) in function of weld size a_w (mm) for longitudinal welds, downhand position

Weld type	Welding method	a_w (mm)	$10^3 T_2 = 10^3 C_2 a_w''$
fillet	SMAW	2-5	$4.0 a_w$
		5-15	$0.8 a_w^2$
fillet	GMAW-C	2-5	$1.70 a_w$
		5-15	$0.34 a_w^2$
fillet	SAW	2-5	$1.190 a_w$
		5-15	$0.238 a_w^2$
1/2 V butt	SMAW	4-15	$0.600 a_w^2$
1/2 V butt	GMAW-C	4-15	$0.257 a_w^2$
1/2 V butt	SAW	4-15	$0.181 a_w^2$
I-butt double-sided	GMAW-C	2-8	$2(0.567 + 0.417 a_w)$

The ratio of k_f/k_m may vary in the range of 0-1.5, the value of $k_f/k_m = 0$ corresponds to the minimum weight design.

4.9.3 DESIGN AND COST CALCULATION OF STRUCTURAL PARTS

4.9.3.1 ROOF

In our numerical example treated in Section 4.9.4 the radius R is varied in the range of $R = 2.9 - 4.25$ m. For these radii a relatively simple roof structure can be used consisting of radial rafters of rolled I-section and trapezoidal plate segments welded to rafters and to inner and outer ring by fillet welds.

The snow load p_s (kN/m^2) acts on roof and the plate elements should be checked for bending. The number of rafters or plate elements can be determined from the restriction that the maximal plate width should not exceed 2.3 m to be transportable. Thus, the number of rafters is $n_r = 2R\pi / 2.3$ rounded up to the next even number.

In an approximate calculation a plate strip can be designed for bending as a simply supported beam with a span length $L_p = 2R\pi / n_r$ and of thickness t_r :

$$\frac{M_{max}}{W_x} = \frac{6\gamma p_s L_p^2}{8t_r^2} \leq f_y \quad (4.9.1)$$

where $\gamma = 1.5$ is the safety factor, $f_y = 355$ MPa is the steel yield stress (for all parts of silo this yield stress is used). Calculating with $p_s = 1$ kN/m² = 10^{-3} N/mm² the required plate thickness from Eq.(4.9.1) is

$$t_r = L_p \sqrt{\frac{3\gamma p_s}{4f_y}} = L_p \sqrt{\frac{0.75 * 1.5 * 10^{-3}}{355}} = 1.78 * 10^{-3} L_p \quad (4.9.2)$$

With the maximal value of $L_p = 2300$ mm, $t_r = 4$ mm. This thickness is used for all radii.

A rafter can be calculated approximately as a simply supported beam having span length of $L_r = R - d_r / 2$, where $d_r = 800$ mm is the diameter of inner ring. The required section modulus is

$$W_x = \gamma M_{max} / f_y = \gamma p_s L_p L_r^2 / (8f_y) \quad (4.9.3)$$

where $\gamma = 1.5$, $f_y = 355$ MPa, $p_s = 10^{-3}$ MPa, $L_p = 2300$ mm.

The self weight of n_r plate elements can be calculated taking an element as a triangle with a width of $2R\pi / n_r$ and length $(R - d_r / 2) / \cos \alpha_r$ ($\alpha_r = 30^\circ$ is the roof slope angle):

$$G_p = \rho_s t_r n_r \pi R (R - d_r / 2) / 0.866 \quad (4.9.4)$$

where $\rho_s = 7850 \text{ kg/m}^3$ is the density of steel.

The self weight of n_r rafters with length $L_r / \cos 30^\circ$ and cross-section area $A \text{ (mm}^2\text{)}$ is

$$G_{raf} = \rho_s n_r A L_r / \cos 30^\circ \quad (4.9.5)$$

The total weight of a roof structure is

$$G_r = G_p + G_{raf} \quad (4.9.6)$$

The fabrication time of the roof is

$$\sum T_i = C_1 \Theta_r \sqrt{\kappa_r G_r} + \sum C_{2n} a_{wri}^n L_{wri} \quad (4.9.7)$$

where $C_1 = 1.0 \text{ min/kg}^{0.5}$, $\Theta_r = 3$, $\kappa_r = 2n_r$; according to COSTCOMP data, for

$a_{wri} = 3 \text{ mm}$ and for GMAW-C welding method $C_{2r} = 1.7 \cdot 10^{-3} \text{ min/mm}^2$, $n = 1$.

The weld length is the sum of perimeters of the inner and outer ring as well as the length of longitudinal welds, approximately

$$L_{wr} = d_r \pi + 2R\pi + 2L_r n_r / \cos 30^\circ. \quad (4.9.8)$$

4.9.3.2 BIN

The circular cylindrical bin is loaded by the horizontal pressure of the stored material calculated with the Janssen's formula

$$p_h = p_o \zeta; \quad p_o = \frac{\rho R}{2\mu}; \quad \zeta = 1 - e^{-z/z_o}; \quad z_o = \frac{R}{2\mu k} \quad (4.9.9)$$

where ρ is the density of stored material, μ is the friction coefficient of the material on the wall, z is the depth of stored material above the investigated section, k is the pressure coefficient. Note that the distance $R \tan \alpha_r / 3$ in Fig. 4.9.1 is the possible height of the stored material in roof, this distance is in the following calculation neglected. With these coefficients the frictional stress on wall is

$$q = \mu p_h \quad (4.9.10)$$

and the vertical pressure in bin is

$$p_v = p_h / k \quad (4.9.11)$$

The circumferential membrane force in bin is

$$n_{\phi b} = p_h R \quad (4.9.12)$$

and the meridional membrane force is

$$n_{zb} = \int_0^z p_v dz = \mu p_o z_o \left(\frac{z}{z_o} - \zeta \right) \quad (4.9.13)$$

The required bin thickness t_b can be calculated from the stress constraint

$$\sigma = \gamma_{red} n_{red} / t_b \leq f_y; \quad n_{red} = \sqrt{n_{\phi b}^2 + n_{zb}^2 + |n_{\phi b} n_{zb}|}$$

$$t_{b \max} = \frac{\gamma_{red} p_o R}{f_y} \sqrt{\zeta_H^2 + \frac{1}{4k^2} \left(\frac{H}{z_o} - \zeta_H \right)^2 + \frac{\zeta_H}{2k} \left(\frac{H}{z_o} - \zeta_H \right)} \quad (4.9.14)$$

where $\zeta_H = 1 - e^{-H/z_o}$ and γ_{red} is the safety factor considering the approximate self weight (0.1*1.35), the dynamic effects of filling and emptying (1.2*1.5) as well as the sudden change of temperature (0.2)

$$\gamma_{red} = 0.1 * 1.35 + 1.2 * 1.5 + 0.2 = 2.135 \quad (4.9.15)$$

The bin thickness is limited to $t_{b \min} = 4 \text{ mm}$ by the fabrication requirements. When the t_b calculated from Eq. (4.9.14) exceeds 4 mm, the thickness can be decreased step by step to 4 mm, since the bin is welded from shell courses. The width of courses is determined by the available plate width (e.g. 1500 mm).

The whole bin should be checked for local buckling due to wind acting on the empty silo. For a cylindrical shell with variable thickness the German standard for steel structures DIN 18800 Part 4 (1990) gives a complicated method. Instead of this method the API 650 formula can be used (Gaylord [4.47])

$$\frac{H}{t_b} \leq 7200 \left(\frac{600 t_b}{R} \right)^{2/3} \quad (4.9.16)$$

where t_b is the average bin thickness.

The constraint on local buckling of bin courses due to the vertical pressure according to DIN 18800 Part 4 is expressed by

$$\sigma_z = 1.1 n_{zb} / t_b \leq \kappa_1 f_y / \gamma_M \quad (4.9.17)$$

where $\gamma_M = 1.1$ is a safety factor, κ_1 is the buckling coefficient

$$\kappa_1 = 1 \quad \text{for } \bar{\lambda}_s \leq 0.4$$

$$\kappa_1 = 1.274 - 0.686 \bar{\lambda}_s \quad \text{for } 0.4 < \bar{\lambda}_s < 1.2 \quad (4.9.18)$$

$$\kappa_1 = 0.65 / \bar{\lambda}_s^2 \quad \text{for } 1.2 \leq \bar{\lambda}_s$$

$$\bar{\lambda}_s = \sqrt{f_y / \sigma_{z, id}}; \quad \sigma_{z, id} = 0.605 E t_b / R$$

With the value of the elastic modulus $E = 2.1 \cdot 10^5 \text{ MPa}$ and for $f_y = 355 \text{ MPa}$ it is

$$\bar{\lambda}_s = \sqrt{\frac{R}{t_b}} \sqrt{\frac{f_y}{0.605E}} = \frac{1}{18.9179} \sqrt{\frac{R}{t_b}} \quad (4.9.19)$$

In our numerical example treated in Section 4.9.4, the required maximal bin thickness is $t_b = 4 \text{ mm}$, so all bin plate elements have the same thickness, 4 mm. Thus, the self weight of the bin is

$$G_b = 2R\pi H \rho t_b \quad (4.9.20)$$

The difficulty factor is taken as $\Theta_b = 4$, since the bin is a spatial structure and needs a special erection method. The bin courses are welded from plate units having dimensions of $6000 \cdot 1500 \text{ mm}$ with horizontal and vertical double-sided I-welds with GMAW-C welding method. Number of courses is $n_{co} = H^{(m)} / 1.5$, the length of circumferential welds is $2R\pi n_{co}$, number of vertical welds is $n_v = 2R^{(m)}\pi / 6.0$ rounded up to the next integer value, length of a vertical weld is 1.5 m. Number of assembled elements is $\kappa_b = 2R\pi n_{co} / 6$.

Thus, the total fabrication time for the bin is given by

$$\sum T_{bi} = \Theta_b \sqrt{\kappa_b G_b} + 1.3 \cdot C_{2b} a_{wb} L_{wb} \quad (4.9.21)$$

where $a_{wb} = 4 \text{ mm}$, $L_{wb} = 2R\pi n_{co} + n_v H$. According to COSTCOMP (Table 4.9.1.) for I-weld welded from both sides $10^3 C_{2b} a_{wb} = 2(0.567 + 0.417 \cdot 4) = 4.4 \text{ min/mm}$.

4.9.3.3 HOPPER

The load component perpendicular to the conical hopper wall can be calculated according to DIN 1055 Part 6 (1987)

$$p' = \left(p_v c_b \sin^2 \beta + p_h \cos^2 \beta \right) \left[1 + \frac{\sin 2(90 - \beta)}{4\mu} \right] \quad (4.9.22)$$

where $c_b = 1.5$, β is the slope angle of hopper (Fig. 4.9.1).

The hoop (circumferential) membrane tension force is

$$n_h = p' R / \cos \beta \quad (4.9.23)$$

The meridional tension is given by Gaylord [4.47] p.271)

$$n_m = \frac{p_v R}{2 \cos \beta} + \frac{Q_m}{2R\pi \cos \beta} \quad (4.9.24)$$

where Q_m is the weight of stored material below the junction of hopper and ringbeam

$$Q_m = \frac{\rho\pi}{24} (8R^3 - d_h^3) \cot\beta$$

d_h is the diameter of the bottom ring of the hopper.

The required hopper wall thickness t_h can be obtained from the stress constraint

$$\sigma_h = \frac{\gamma_h n_{red.h}}{t_h} \leq f_y; \quad n_{red.h} = \sqrt{n_h^2 + n_m^2 - n_h n_m} \quad (4.9.25)$$

$$\gamma_h = 1.5.$$

The self weight of the hopper is expressed by

$$G_h = \frac{\rho_s \pi}{\sin\beta} \left[R^2 - \left(d_h / 2 \right)^2 \right] t_h \quad (4.9.26)$$

The number of plate elements is the same as in the case of roof $\kappa_h = 2R\pi / 2.3$. The difficulty factor is taken as $\Theta_h = 4$, since the hopper is fabricated from shell elements. The hopper thickness is for all silos treated in Section 4 $t_h = 4\text{mm}$, so for I-welds between shell elements $10^3 C_{2h1} a_{wh} = 4.4 \text{ min/mm}$. The length of a weld is $L_{wh1} = (R - d_h / 2) / \sin\beta$, the total length is $L_{wh1} \kappa_h$. The hopper is welded to the ringbeam by two circumferential fillet welds of size $a_w = 4\text{mm}$, for which $C_{2h2} = 1.7 * 10^{-3} \text{ min/mm}^2$, and the length of welds is $L_{wh2} = 4R\pi$. Thus, the total fabrication time for hopper is given by

$$\sum T_{hi} = \Theta_h \sqrt{\kappa_h G_h} + 1.3 \left(C_{2h1} L_{wh1} \kappa_h + 4 C_{2h2} L_{wh2} \right) \quad (4.9.27)$$

4.9.3.4 COLUMNS

Columns are loaded by self weight of roof, bin, hopper and ringbeam as well as by snow, wind and weight of the stored material. In the case of more variable actions EC 3 prescribes two combinations as follows: a) considering only the most unfavourable variable action (Q) adding to the permanent actions (G): $\sum_j G_j + Q_1$; b) considering all

unfavourable variable actions multiplied by 0.9: $\sum_j G_j + 0.9 \sum_i Q_i$. The safety factor is

$\gamma = 1.35$ for G and $\gamma = 1.5$ for Q .

The number of columns (n_{col}), as mentioned in the introduction, is limited by the transit function of the silo and the minimal number of columns is 6.

The snow load, according to Section 4.9.3.1 is $Q_{snow} = \pi R^2 p_s$. The weight of the stored material is $Q_{stor} = \rho V_{stor}$, the volume is given by

$$V_{stor} = \pi R^2 H + \pi H_h \left(\frac{d_h}{2} \right)^2 + \frac{\pi}{3} H_h \left(R - \frac{d_h}{2} \right)^2; \quad H_h = \left(R - \frac{d_h}{2} \right) \cot \beta \quad (4.9.28)$$

In our numerical example the weight of stored material gives the leading combination, so the effect of snow and wind can be neglected. Note that the effect of earthquake load is treated in Section 4.9.5.

The compressive force of a column is

$$N_c = \frac{1}{n_{col}} \left(1.35 \sum_j G_j + 1.5 Q_{stor} \right) \quad (4.9.29)$$

The overall buckling constraint is expressed by

$$N_c / A_c \leq \chi f_y \quad (4.9.30)$$

In the case of columns of square hollow section of width b_c and thickness t_c , $A_c = 4b_c t_c$. The length of a column with pinned ends is $L_c = H_h + 2m$.

The buckling coefficient can be calculated on the basis of the JRA (Japanese Road Association) column curve which gives values similar to EC 3 curve "b":

$$\begin{aligned} \chi &= 1 & \text{for } \bar{\lambda}_c \leq 0.2 \\ \chi &= 1.109 - 0.545 \bar{\lambda}_c & \text{for } 0.2 < \bar{\lambda}_c < 1 \\ \chi &= \frac{1}{0.773 + \bar{\lambda}_c^2} & \text{for } \bar{\lambda}_c \geq 1 \end{aligned} \quad (4.9.31)$$

The reduced slenderness is defined by

$$\bar{\lambda}_c = \frac{L_c \sqrt{6}}{b_c \lambda_E}; \quad \lambda_E = \pi \sqrt{\frac{E}{f_y}} = 76.41$$

The local buckling constraint according to EC 3 is

$$\delta_c = b_c / t_c \leq \delta_{cL} = 42 \varepsilon = 34; \quad \varepsilon = \sqrt{235 / f_y}, \quad (f_y \text{ in MPa}) \quad (4.9.32)$$

Treating Eq. (4.9.32) as active, the cross-sectional area can be expressed as

$$A_c = 4b_c t_c = 4b_c^2 / \delta_{cL} \quad (4.9.33)$$

Assuming that $0.2 < \bar{\lambda}_c < 1$, Eq. (4.9.30) can be written as

$$\frac{N_c}{f_y} = \chi A_c = \left(1.109 - 0.545 \frac{L_c \sqrt{6}}{b_c \lambda_E} \right) \frac{4b_c^2}{\delta_{cL}} \quad (4.9.34)$$

which is a quadratic equation for b_c .

The self weight of columns is

$$G_{col} = \rho_s n_{col} A_c L_c \quad (4.9.35)$$

Since the sections are not welded, the fabrication cost of columns may be neglected.

It should be noted that, for the spatial stability of a silo, wind braces are needed between columns. The cost of these braces is neglected.

4.9.3.5 RINGBEAM

The loads acting on the transition ringbeam cause compression, bending, shear and torsion. Since the open section beams have very small torsional stiffness, it is advantageous to use a welded box ringbeam [4.50].

The dimensions of the ringbeam can be calculated using the constraints on stress and local buckling of component plates. To construct a suitable connection between columns and ringbeam the distance between the two webs of the box beam should be equal to column width b_c , thus, the flange width will be $b_r = b_c + 40\text{mm}$. Note that this is the reason why we treat the design of the ringbeam after the design of columns.

Since the horizontal component of the tensile force acting from the hopper causes compression in the ringbeam, it is necessary to use in the local buckling constraint of webs the same limiting plate slenderness $\delta_L = 42\varepsilon = 34$ as for flanges. Thus, the active local buckling constraints are as follows:

$$\text{for webs } 2h_r / t_{wr} \leq \delta_L \quad (4.9.36)$$

$$\text{for flanges } b_r / t_{rb} \leq \delta_L \quad (4.9.37)$$

The vertical component of the tensile membrane force acting from the hopper is

$$y_r = \frac{\gamma Q_{stor}}{2R\pi} \quad (4.9.38)$$

This load causes bending and shear in vertical plane of the ringbeam

$$M_{r,max} = y_r L_r^2 / 12; \quad L_r = 2R\pi / n_{col} \quad (4.9.39)$$

The horizontal component

$$x_r = y_r \tan \beta \quad (4.9.40)$$

causes compression

$$n_r = x_r R \quad (4.9.41)$$

The cross-sectional area of the ringbeam is

$$A_r = h_r t_{wr} + 2b_r t_{rb} = 2(h_r^2 + b_r^2) / \delta_L \quad (4.9.42)$$

and the section modulus is expressed by

$$W_{xr} = h_r^2 t_{wr} / 6 + h_r b_r t_{rb} = (h_r^3 + 3h_r b_r^2) / (3\delta_L) \quad (4.9.43)$$

In Eq. (4.9.42) and (4.9.43) the only unknown is h_r , which can be calculated from the stress constraint

$$\frac{M_{r, \max}}{W_{xr}} + \frac{n_r}{A_r} \leq f_y \quad (4.9.44)$$

Unfortunately, a closed formula cannot be derived from Eq. (4.9.44).

The self weight of the ringbeam is

$$G_{rb} = \rho_s 2\pi(R + b_c / 2) A_r \quad (4.9.45)$$

The ringbeam is welded using four fillet welds of dimension $a_w = 4\text{ mm}$. The difficulty factor is $\Theta_{rb} = 4$ since a curved beam should be fabricated.

$\kappa_{rb} = 4$, $C_{2rb} = 1.7 \cdot 10^{-3} \text{ min/mm}^2$. The whole weld length is

$$L_{wrb} = 4R\pi + 4(R + b_c) \quad (4.9.46)$$

The total fabrication time of a ringbeam is

$$\sum T_{rbi} = \Theta_{rb} \sqrt{\kappa_{rb} G_{rb}} + 1.3 \cdot 4 C_{2rb} L_{wrb} \quad (4.9.47)$$

4.9.4 NUMERICAL EXAMPLE

We select the extreme heights $H = 7.5$ and 18.0 m for integer numbers of courses n_{co} . For a given constant storage capacity $V_{\text{stor}} = 500 \text{ m}^3$ the required radius R can be calculated from Eq. (4.9.28). The dimensions, self weights and costs are determined for four silos, i.e. for $H = 7.5, 12.0, 15.0$ and 18.0 m for storage of cement with a density of $\rho = 1600 \text{ kg/m}^3$. For cement it is $\mu = 0.4$ and $k = 0.6$. The density of steel is $\rho_s = 7850 \text{ kg/m}^3$. The data for the cost calculation are summarized in Table 4.9.2.

The results of the calculations are shown in Table 4.9.3. Fig. 4.9.2. shows the results as a function of H/R for $k_f / k_m = 1.5$.

Table 4.9.2. Calculation of fabrication times T_f and $T_2 + T_3$ according to Eq.(4.9.3) and (4.9.6) for structural parts of a welded silo. For all parts $C_1=1.0 \text{ min/kg}^{0.5}$, $n=1$

Structure	roof	bin	ringbeam	hopper
Θ	3	4	4	4
κ	$4R\pi/2300$	$n_{co} n_v$	4	$2R\pi/2300$
G	Eq. (4.9.6)	Eq.(4.9.20)	Eq.(4.9.45)	Eq. (4.9.26)
welds a_w (mm)	fillet, 3	I-weld, 4	fillet, 3	I-weld, 4
C_2 (min/mm ²)	$1.7 \cdot 10^{-3}$	$1.1 \cdot 10^{-3}$	$1.7 \cdot 10^{-3}$	$1.1 \cdot 10^{-3}$
L_w	Eq.(4.9.8)	Eq.(4.9.21)	Eq.(4.9.46)	$\frac{R-d_h/2}{\sin \beta}$
				$4R\pi$

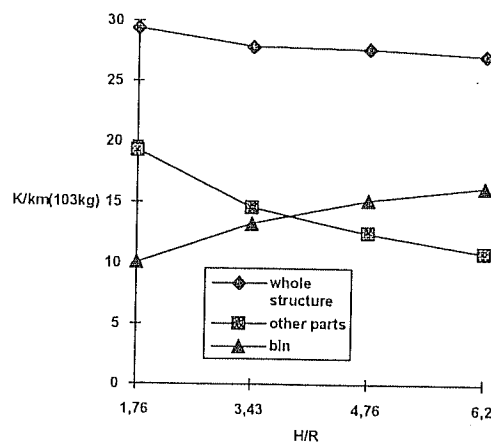


Fig. 4.9.2. Cost of silo parts in the function of H/R for $k_f/k_m=1.5$

4.9.5 CONSIDERATION OF EARTHQUAKE LOAD

When designing silos for earthquake risk zones, a horizontal force should be considered acting in the center of gravity, approximately in the height of $q = L_c + H/2$ (Fig.4.9.1). According to Gaylord ([4.47], p.139) this force can be calculated for bins with above-ground bottoms by the formula

$$V = 0.2ZQ \quad (4.9.48)$$

where Z is the seismic zone coefficient. For instance, for zone 2 (moderate damage, with modified Mercalli scale intensity VII) $Z = 3/8$. Thus,

$$V = 0.075Q \quad (4.9.49)$$

In our numerical example $Q = Q_{stor} = \rho V_{stor} = 8000 \text{ kN}$, $V = 600 \text{ kN}$.

Table 4.9.3. K/k_m (kg) values for four silos of equal storage capacity of 500 m³

$\frac{k_f}{k_m} \left(\frac{\text{kg}}{\text{min}} \right)$	$R(\text{m})$	4.25	3.50	3.15	2.90
	$H(\text{m})$	7.50	12.00	15.00	18.00
	H/R	1.76	3.43	4.76	6.20
0	roof	2181	1449	1176	963
	bin	6289	8286	9322	10299
	ringbeam	4585	3653	3003	2521
	hopper	2747	1855	1498	1266
	columns	2681	2231	2068	1952
	total	18483	17474	17067	17001
1.0	roof	3769	2597	2073	1779
	bin	8853	11627	13240	14295
	ringbeam	6101	4943	4170	3597
	hopper	4356	3065	2583	2169
	columns	2681	2231	2068	1952
	total	25760	24463	24134	23792
1.5	roof	4563	3171	2589	2188
	bin	10135	13297	15199	16293
	ringbeam	6859	5888	4754	4135
	hopper	5160	3670	3125	2620
	columns	2681	2231	2068	1952
	total	29398	28257	27735	27188

The combination of loads in Eq.(4.9.35) should be modified, since the combination of

$$\sum G_j + 0.9 \sum Q_i$$

will be the leading one. The force acting on a column due to V in the case of 6 columns is

$$N_{cV} = \frac{Vq}{4R \cos 30^\circ} \quad (4.9.50)$$

and the total compressive force acting on a column (number of columns $n_c = 6$)

$$N_c = 1.35 \sum G_j / 6 + 0.9 * 1.5 (Q_{stor} / 6 + N_{cV}) \quad (4.9.51)$$

The design of columns should be performed for this N_c . The calculations in our numerical example give the following results. The K/k_m (kg) values in Table 4.9.3. for columns should be modified from the values 2681, 2231, 2068 and 1952 to 3506, 2870, 2809 and 2650, respectively. The other values can remain unchanged since the changes in column dimensions affect the other dimensions only very slightly. The values of the "total" rows should be changed by adding 825, 639, 741 and 582, respectively. It can be seen that the

tendency described below in conclusions does not change in our case when considering the earthquake load.

4.9.6 CONCLUSIONS

For a given storage capacity, including the hopper volume, and for given bin height H , the radius R can be determined. The aim was to find the optimal H/R ratio for a given storage capacity in the practical range of $H/R=1.76-6.20$.

The calculations of an illustrative numerical example show the following.

- 1) When the H/R ratio increases *the self weight* of the bin increases but the self weight of the other parts of silo (roof, ringbeam, hopper and columns) decreases. The self weight of the whole structure has a minimum at the practical upper limit of $H/R = 6.20$. The difference between the self weights of the best and worst solution is $100(18483-17001)/17001 = 9\%$.
- 2) *The material and fabrication cost* of the whole structure decreases when H/R increases and reaches the minimum at the practical upper limit of H/R . Thus, designers have to choose the maximal H/R to achieve minimal costs. The cost difference between the best and worst solution is $100(29398-27188)/27188 = 8\%$.
- 3) The number of columns should be minimal, the practical minimal number is 6. The slope angle of the hopper should be chosen in accordance with the friction angle of the stored material.
- 4) In the design of bin thickness the constraints on reduced stress and local buckling should be considered. The effect of a sudden temperature change as well as the dynamic filling and emptying effects are taken into account by multiplying factors. The thickness of the hopper is determined on the basis of the constraint on reduced stress.
- 5) The optimal dimensions of the ringbeam can be calculated from the stress and local buckling constraints. In the stress constraint the effect of compression and bending should be considered.
- 6) In the design of columns the effect of snow and wind can be neglected, the leading action is the weight of the stored material. This calculation should be modified when the effect of earthquake load is considered (see Section 4.9.5). Simple closed formulae can be derived for the optimal dimensions of columns of square hollow section.

ACKNOWLEDGEMENTS

The authors would like to thank Andre L. Tits and Jian L. Zhou University of Maryland for the possibility of using the CFSQP algorithm.

This work received support from the Hungarian Fund for Scientific Research Grants OTKA T-4479 and T- 019003.

REFERENCES

- 4.1 Walker, R.J.: An enumerative technique for a class of combinatorial problems, in: Proc. of Symposia in Appl. Math. Amer. Math. Soc. Providence, R.I. 10(1960), 91-94.
- 4.2 Golomb, S.W. and L.D. Baumert: Backtrack programming, J. Assoc. Computing Machinery, 12 (1965), 516-524.
- 4.3 Bitner, J.R. and E.M. Reingold: Backtrack programming techniques, Communications of ACM, 18(1975), 651-656.
- 4.4 Lewis, A.D.M.: Backtrack programming in welded girder design, in: Proc. 5th Annual SHARE-ACM-IEEE Design Automation Workshop, Washington, 1968, 28/1-28/9.
- 4.5 Annamalai, N.: Cost optimization of welded plate girders. Dissertation, Purdue Univ. Indianapolis, Ind. 1970.
- 4.6 Farkas, J. and L. Szabó: Optimum design of beams and frames of welded I-sections by means of backtrack programming. Acta Techn. Hung. 91(1980), 121-135.
- 4.7 Knuth, D.E.: Estimating the efficiency of backtrack programs. Mathematics of Computation 29(1975), 121-136.
- 4.8 Farkas, J.: Optimum Design of Metal Structures. Akadémiai Kiadó, Budapest, Ellis Horwood, Chichester, 1984.
- 4.9 Jármai, K.: Optimal design of welded frames by complex programming method. Publ. Techn. Univ. Heavy Ind. Ser. C. Machinery, 37(1982), 79-95.
- 4.10 Farkas, J.: Cost comparisons of plates stiffened on one side and cellular plates. Welding in the World 30(1992), 132-137.
- 4.11 Pahl, G. and K.H. Beelich: Kostenwachstumsgesetze nach Ähnlichkeitsbeziehungen für Schweissverbindungen, in: VDI-Bericht Nr. 457. 1982, Düsseldorf, 129-141.
- 4.12 Farkas, J.: Discussion to "Simplified analysis for cellular structures" by Evans, H.R. and Shanmugam, N.E.: J. Struct. Eng. ASCE 111(1985), 2268-2271.
- 4.13 Timoshenko, S. and S. Woinowsky-Krieger: Theory of plates and shells. 2nd ed. McGraw Hill, New York-Toronto-London, 1959.
- 4.14 Usami, Ts. and Y. Fukumoto: Local and overall buckling of welded box columns. J. Struct. Div. Proc. ASCE (1982), 525-541.
- 4.15 Zhou, J.L. and A. Tits: User's guide for FSQP Version 3.0: a Fortran code for solving optimization problems. Systems Research Center, University of Maryland, Techn. Report SRC-TR-90-60 rlf, College Park. 1992.
- 4.16 Farkas, J.: Minimum cost design of tubular trusses considering buckling and fatigue constraints, in: Tubular Structures. 3rd Int. Symposium, 1989, Lappeenranta, E. Niemi, P. Mäkeläinen (eds), Elsevier, London, 1990, 451-459.
- 4.17 Farkas, J.: Techno-economic considerations in the optimum design of welded structures. Welding in the World 29(1991), 295-300.
- 4.18 Farkas, J. and K. Jármai: Minimum cost design of laterally loaded welded rectangular cellular plates. In Structural Optimization '93 World Congress, Rio de Janeiro. Proc. Vol. 1. 1993, 205-212.

- 4.19 Ott, H.H. and V. Hubka: Vorausberechnung der Herstellkosten von Schweisskonstruktionen. (Fabrication cost calculation of welded structures), in: Proc.Int.Conference on Engineering Design ICED, 1985. Hamburg. Ed. Heurista, Zürich, 1985, 478-487.
- 4.20 COSTCOMP, Programm zur Berechnung der Schweisskosten. Deutscher Verlag für Schweißtechnik, Düsseldorf, 1990.
- 4.21 Bodt, H.J.M.: The global approach to welding costs. The Netherlands Institute of Welding, The Hague, 1990.
- 4.22 American Petroleum Institute: API Bulletin on Design of flat plate structures. Bul. 2V, 1st. ed. 1987.
- 4.23 Eurocode 3. (EC3) Design of steel structures. Part 1.1. Brussels, CEN - European Committee for Standardization, 1992.
- 4.24 Khot, N.S. and L. Berke: Structural optimization using optimality criteria methods, in: New directions in optimum structural design. Eds. Atrek, E., Gallagher, R.H. et al. Wiley & Sons, Chichester, New York, etc. 1984, 47-74.
- 4.25 Vanderplaats, G.N. and F. Moses: Automated design of trusses for optimum geometry. Journal of Structural Division Proc. ASCE 98(1972), 671-690.
- 4.26 Saka, M.P.: Shape optimization of trusses. Journal of Structural Division Proc. ASCE 106(1980), 1155-1174.
- 4.27 Amir, H.M. and T. Hasegawa: Shape optimization of skeleton structures using mixed-discrete variables. Structural Optimization 8(1994), 125-130.
- 4.28 Farkas, J.: Optimum design of circular hollow section beam-columns, in: Proceedings of the Second International Offshore and Polar Engineering Conference, San Francisco, 1992. ISOPE, Golden, Colorado, USA. 494-499.
- 4.29 Saka, M.P.: Optimum design of pin-jointed steel structures with practical applications. Journal of Structural Division Proc. ASCE 116(1990), 2599-2620.
- 4.30 Farkas, J. and K. Jármai: Savings in weight by using CHS or SHS instead of angles in compressed struts and trusses, in: Tubular Structures VI. Proceedings of the 6th International Symposium, Melbourne, 1994. Eds. Grundy, P., Holgate, A., Wong, B. Balkema, Rotterdam - Brookfield. 417-422.
- 4.31 Dutta, D. and K-G. Würker: Handbuch Hohlprofile in Stahlkonstruktionen. Köln, TÜV Rheinland GmbH, 1988.
- 4.32 Wardenier, J., Kurobane, Y. et al.: Design guide for circular hollow section joints under predominantly static loading. Köln, TÜV Rheinland, 1991.
- 4.33 Rondal, J., Würker, K-G. et al.: Structural stability of hollow sections. Köln, TÜV Rheinland, 1992.
- 4.34 Saka, M.P.: Optimum geometry design of roof trusses by optimality criteria method. Computers & Structures 38(1991), 83-92.
- 4.35 Koumoussis, V.K.: Lay-out and sizing design of civil engineering structures in accordance with the Eurocodes, in: Topology Design of Structures. Eds. Bendsoe, M.P. & C.A. Mota Soares. Dordrecht-Boston-London: Kluwer: 1992, 103-116.

- 4.36 Packer, J.A., J. Wardenier et al., Design guide for rectangular hollow section joints under predominantly static loading. Köln: TÜV Rheinland, 1992.
- 4.37 Hasegawa, A., H. Abo et al., Optimum cross-sectional shapes of steel compression members with local buckling, in: Proc. JSCE Structural Engineering/ Earthquake Engineering 2(1985), 121-129.
- 4.38 Eschenauer, H., Koski, J. and Osyczka, A., Multicriteria Design Optimization. Springer, Berlin, etc. 1990.
- 4.39 Koski, J.: Bicriterion optimum design method for elastic trusses. Acta Polytechnica Scandinavica, Mechanical Engineering Series No.86. Helsinki, 1984.
- 4.40 Osyczka, A.: Multicriterion Optimization in Engineering. Ellis Horwood, Chichester, 1984.
- 4.41 Farkas, J.: Fabrication aspects in the optimum design of welded structures. Structural Optimization 4(1991), 51-58.
- 4.42 Jármai, K.: Single- and multicriteria optimization as a tool of decision support system. Computers in Industry 11(1989), 249-266.
- 4.43 Jármai, K.: Application of decision support system on sandwich beams verified by experiments. Computers in Industry 11(1989), 267-274.
- 4.44 Jármai, K.: Decision support system on IBM PC for design of economic steel structures, applied to crane girders. Thin-walled Structures 10(1990), 143-159.
- 4.45 Farkas, J. and K. Jármai: Multiobjective optimal design of welded box beams. Microcomputers in Civil Engng 10(1995), 249-255.
- 4.46 Martens, P. ed.: Silo-Handbuch. Berlin, Ernst & Sohn, 1988.
- 4.47 Gaylord, E.H. jr. and Gaylord, Ch.N.: Design of steel bins for storage of bulk solids. Prentice Hall, Inc. Englewood Cliffs, New Jersey, 1984.
- 4.48 Trahair, N.S., Abel, A. et al.: Structural design of steel bins for bulk solids. Australian Institute of Steel Construction, Sydney, 1983.
- 4.49 Teng, J.G. and J.M. Rotter: Recent research on the behaviour and design of steel silo hoppers and transition junctions. Journal of Constructional Steel Research, 23(1992), 313-343.
- 4.50 Farkas, J.: Discussion to "Elastic behaviour of isolated column-supported ringbeams" by Rotter, J.M.- J. Constructional Steel Research 4(1984), 235-252. J.C.S.R. 5(1985), 239-242.